Ion-water and ion-polypeptide correlations in a gramicidin-like channel

A molecular dynamics study

Peter C. Jordan
Department of Chemistry, Brandeis University, Waltham, Massachusetts 02254-9110 USA

ABSTRACT This work describes a molecular dynamics study of ion-water and ion-polypeptide correlation in a model gramicidin-like channel (the polyglycine analogue) based upon interaction between polarizable, multipolar groups. The model suggests that the vicinity of the dimer junction and of the ethanolamine tail are regions of unusual flexibility. Cs^+ binds weakly in the mouth of the channel: there it coordinates five water molecules and the #11 CO group with which it interacts strongly and is ideally aligned. In the channel interior it is generally pentacoordinate; at the dimer junction, because of increased channel flexibility, it again becomes essentially hexacoordinate. The ion is also strongly coupled to the #13 CO but not to either #9 or #15, consistent with ^{13}C NMR data. Water in the channel interior is strikingly different from bulk water; it has a much lower mean dipole moment. This correlates with our observation (which differs from that of previous studies) that water-water angular correlations do not persist within the channel, a result independent of ion occupancy or ionic polarity. In agreement with streaming potential measurements, there are seven single file water molecules associated with Cs^+ permeation; one of these is always in direct contact with bulk water. At the mouth of an ion-free channel, there is a pattern of dipole moment alternation among the polar groups. Due to differential interaction with water, exo-carbonyls have unusually large dipole moments whereas those of the endo-carbonyls are low. The computed potential of mean force for Cs^+ translocation is qualitatively reasonable. However, it only exhibits a weakly articulated binding site and it does not quantitatively account for channel energetics. Correction for membrane polarization reduces, but does not eliminate, these problems.

INTRODUCTION

A number of questions are basic to developing a theoretical understanding of the process of ion permeation through transmembrane channels. One should be able to relate a channel's molecular structure to its turnover capacity, its selectivity sequence and its gating characteristics. Even with recent developments in protein design (DeGrado et al., 1989), in the synthesis of polypeptide fragments which mimic channel behavior (Oiki et al., 1988), in the possible identification of channel gates (Stühmer et al., 1989) or in the modeling of permeation energy profiles (Åqvist and Warshel, 1989), theory is far from attaining this goal (Jordan, 1987).

The qualitative features that must account for biological ion channels' exceptional ability to selectively facilitate translocation of ions across membranes have often been described (Hille, 1984). Narrow pore interiors, lined with charged or polar groups, and in which permeant motion proceeds in a single file, provide an environment which stabilizes water and some charged species. Selectivity involves a delicate energetic balancing act. The relative affinity of an ion for water and the channel interior cannot differ too much; furthermore, the energy barriers to ion entry or translocation cannot be too great. If these conditions are not satisfied, an ion cannot permeate; it will either block the channel or not enter it. The whole process of ion permeation can be pictured in terms of seven distinct primitive steps: diffusion to the channel entrance; association with the channel; entry into the single file domain; diffusion across the channel; exit from the single file region; dissociation from the channel; diffusion away from the channel exit. It is the five intermediate steps that require the ion to undergo the most substantial changes in its solvation structure. In association the ion loses part of its inner hydration shell and associates with polar groups lining the mouth of the channel. Entry into the single file domain completes the dehydration process. In internal diffusion, depending upon the length of the single file region, the ion is transferred between polar groups of the channel interior, processes which require repeated alterations in its solvation structure. Exiting and dissociation reverse the first two steps and rehydrate the ion.

Physiologically active channels are integral membrane proteins which typically have several thousand amino acid residues (Noda et al., 1983, 1984). Even when primary sequences are known, relatively little high resolution structural data are available. Theoretical studies of ion permeation at the molecular level have of necessity focussed on simpler channel forming proteins. The pentadecapeptide gramicidin A and its analogues are small channel forming proteins, readily amenable to chemical

modification, and relatively easily studied electrophysiologically (Andersen, 1984); they are ideal systems for this purpose. Theoretical models have been constructed to mimic features of the dimeric channel former; these treatments ignore or seriously oversimplify the influence of the phospholipid membrane on the permeation properties of the gramicidin dimer. The microscopic calculations include applications of Monte Carlo methods (Fornili et al., 1984; Kim and Clementi, 1985; Kim et al., 1985), quantum chemistry (Pullman and Etchebest, 1983; Etchebest and Pullman, 1984, 1986; Etchebest et al., 1984; Pullman, 1987), molecular dynamics (Mackay et al., 1984; Mackay, D. H. J., P. M. Edelstein, and K. R. Wilson, unpublished results; Chiu et al., 1989), molecular mechanics coupled to a mean field theory of long range interactions (Åqvist and Warshel, 1989), energy minimization and molecular dynamics of gramicidin's polyglycine analogue (Lee and Jordan, 1984; Sung and Jordan, 1987; Jordan, 1988), and molecular dynamics of a helically periodic abstraction of gramicidin (Polymeropoulos and Brickmann, 1985; Skerra and Brickman, 1987*a*, *b*). Each uses a different model potential to describe the system and approximates it differently. Each emphasizes distinct aspects of water and/or ion interaction with the protein: association with the mouth of the channel; effect of the ethanolamine and chain's flexibility; interactions in the channel interior; orientational and translational dynamical correlations. Recent studies have also modeled the effect of transmembrane potentials on ion transport (Skerra and Brickmann, 1987*b*) and, by treating long range interactions using a mean field formalism, have accounted for some of the differences between the aqueous and membrane environments (Åqvist and Warshel, 1989). These studies, by focusing attention on the details of the competitive resolvation that occurs during the permeation process, provide insights generally applicable to transport in physiological channels.

Our approach to studying ion interaction with the gramicidin channel contrasts notably with that used by other groups. The molecular model is structurally a bit unusual in that the amino acid residues are ignored and the helical dimer is described by its polyglycine analogue. While changing the amino acid sequence has well-documented effects on the electrical properties of the channel (Heitz et al., 1982; Mazet et al., 1984; Urry et al., Durkin et al., 1986; Barrett-Russell et al., 1986; Koeppe et al., 1988; Andersen et al., 1988), the helical peptide backbone is a major determinant of the channel's ability to facilitate ion transport. The model is analogous to the periodic dipolar helix studied by Brickmann's group (Fischer et al., 1981; Polymeropoulos and Brickmann, 1985; Skerra and Brickmann, 1987*a*, *b*); unlike theirs, ours is finite and incorporates a channel-water interface. The treatment is computationally different; we focus on polar groups and explicitly include polarization interactions. This latter may be especially important in describing the single file region of the channel. Water in a pore has a dramatically different local electrostatic environment than bulk water. Its electrical properties may not be adequately described by models designed to reproduce the mean properties of bulk water.

I present a model of the channel and a way to describe the lipid. The potential function, and the correspondence between group-based and atom-based descriptions are discussed, and the simulational procedure is outlined. Umbrella sampling methods (Pangali et al., 1979) are used to construct a potential of mean force (PMF) for Cs^+ permeation and to model the ion-free channel and a channel with Cl^- at the mouth. The various computations yield structural data illustrating how ionic valence affects resolvation during the translocation process. We consider the effect of ionic polarity on helix structure, especially near the channel mouth; the influence of both helix and ion on channel water's electrical properties; water-water and ion-water correlations in selected regions of the channel; possible ways to identify the single file region, ion-helix correlation; and changes in cation coordination during translocation.

As this model differs sharply from that used in other studies, differences between our predictions and those of previous investigators are to be expected. Where the predictions agree, it argues that the conclusions, being model independent, are basically valid. Where they don't, it suggests areas of investigation needing further detailed study.

MODEL

Analogue gramicidin channel

The crystal structure of the predominant electrically active form of gramicidin is unknown.[1] The handedness of the helix is still an open question, although recent work strongly favors right-handedness (Urry, 1971; Urry et al., 1982*b*; Arseniev et al., 1985; Etchebest and Pullman, 1988; Cornell et al., 1988; Cornell and Separovic, 1989; Nicholson and Cross, 1989; Andersen et al., 1990). The model used here is the polyglycine analogue of the left-handed helical dimer of gramicidin which incorporates major qualitative features essential to understand-

[1]The crystal structure of a gramicidin-salt complex is known (Wallace and Ravikumar, 1988); however this pore, which is a dimer stable in organic solvent (Wallace, 1986) and possibly a minor conducting form (Durkin et al., 1987), has an anti-parallel double stranded conformation. The electrically active form is almost certainly an N-terminus to N-terminus helical dimer, similar to that proposed intially by Urry (1971).

ing gramicidin's electrical conductance (Lee and Jordan, 1984; Sung and Jordan, 1987; Jordan, 1987, 1988). Conformational analysis provides a reasonable set of coordinates for the backbone atoms of the model channel (Koeppe and Kimura, 1984). Monomers are joined at the N-termini via 6 interhelical hydrogen bonds. The CHO residue at the N-terminus is numbered 0 and the COH of the ethanolamine residue is numbered 16. All but three carbonyl oxygens (#11, 13, and 15) form intra- or intermonomer hydrogen bonds.

System geometry

The model geometry has been described previously (Jordan, 1988). "Bulk water" is approximated by hemispherical regions of radius 18 Å at each end of the channel; 419 water molecules are used. Water is constrained by reflection at the hemispherical walls. The density of the water in the "bulk" domains is variable. In the region from 0 to 10 Å from the channel mouth it is roughly that of liquid water; further from the mouth it decreases gradually.[2] The channel is embedded in a "lipid-like" domain of 589 randomly distributed immobile force centers with the approximate size of CH_2 groups in a cylindrical region of 15 Å radius. This approximation was chosen for simplicity and because the proper way to simulate a water-phospholipid interface is still unanswered (Jonsson et al., 1986). The "lipid" has two useful features. It constrains the gramicidin helix and provides an extra pathway for energy transfer between the regions containing bulk water and the channel with its incorporated ion and waters.

THEORY

Potential energy

The model potential contains five terms: electrostatic, Lennard-Jones, bond polarization, backbone deformation, and group localization contributions (Lee and Jordan, 1984; Sung and Jordan, 1987). It differs from standard molecular force fields such as AMBER (Weiner et al., 1984), CHARMM (Brooks et al., 1983), or GROMOS (Hermans et al., 1984) in two significant ways: the basic units are uncharged, dipolar moieties (H_2O, CO, and NH), rather than individual atoms; each of our groups is polarizable. This approach can accommodate charge redistribution that occurs due to ion-group and group-group interactions, which may be important in modeling the properties of water in a pore environment, a state in which its surroundings are vastly different from those in bulk water. The standard force fields describe all water molecules as average bulk waters; as such they do not allow for the possibility that the water molecules may have different molecular properties (e.g., dipole moments) in different surroundings.

TABLE 1 Bare dipole moments, μ_o, and polarizabilities, α, of constituent groups

Group	μ_o/Debye	$\alpha/\text{Å}^3$
CO	2.17*	1.82
NH	0.96	1.44
C_α	0.00	1.84
H_2O	1.86‡	1.44
Cs^+	0.00	2.86§
Cl^-	0.00	2.16

*Helix group parameters from Pethig (1979).
‡Water parameters from Shepard et al. (1973) and Neumann and Moskowitz (1968).
§Ion parameters from Gowda and Benson (1982).

Water, the groups of the gramicidin backbone and the ion are described as polarizable multipoles embedded in Lennard-Jones spheres. Uncompensated dipole moments and polarizabilities are those used previously (Sung and Jordan, 1987) and are listed in Table 1. The forces, torques, and electric fields depend on the interaction between all groups separated by less than a preselected cutoff distance; however, near neighbors in a particular monomer are not coupled via the nonbonded forces (electrical and Lennard-Jones). In standard treatments, the nonbonded interactions between atoms in a particular protein are forbidden unless atoms are separated by more than two (Mackay et al., 1984) or three intervening atoms (McCammon et al., 1979; van Gunsteren and Karplus, 1982). Within individual monomer helices, nonbonded interaction of neighbor and second neighbor groups is forbidden.[3] This is a compromise because interacting protein atoms can then be separated by as few as two to as many as four intervening ones. As an example, successive carbonyl C's interact even though they are separated by only two atoms. On the other hand, an amino H does not interact with the O of the subsequent carbonyl even though these atoms are separated by three intervening atoms.

Lennard-Jones 6-12 parameters σ and ϵ for homo-group

[2]This approximation is used to avoid requiring periodic boundary conditions with an attendant increase in computational complexity. By letting the density fall off near the wall, we also avoid the danger of creating spurious structural correlations in the water phases.

[3]This is different from the exclusion principle used previously, in which second neighbor groups were allowed to interact (Lee and Jordan, 1984; Sung and Jordan, 1987). For finite temperature studies it is necessary to extend the exclusion zone because the thermal motion permits excessively strong coupling between second neighbors.

interaction among backbone groups were derived from Hagler's atom-based values (Mackay et al., 1984); they are measures of group size and ease of compression, respectively. The parameters for CH_2 are identical to those for C_α. Interaction energetics with NH and CO are dominated by N and O atom contributions, respectively. Consequently, the ϵ's for N and O describe NH and CO groups and the σ's for N and O, shifted to account for the distance between an atomic center and a group center-of-mass, describe NH and CO groups. Lennard-Jones parameters for water and for water-ion interaction are those used previously (Barnes et al., 1979; Sung and Jordan, 1986). Hetero-group and ion-group parameters are estimated using geometrically weighted combination rules (Kong, 1973). The parameter set is listed in Table 2.

The interaction between the "lipid-like" force centers and *all* other groups is a Lennard-Jones potential with $\epsilon = 0.59$ kJ mol^{-1} and $\sigma = 3.46$ Å, typical of CH_2-water interaction (Lee et al., 1984). The bond polarization energy, $\frac{1}{2}\Sigma\alpha_i E_i^2$, with E_i the electric field at group i, is the energy required to create the induced dipoles (Landau and Lifschitz, 1960). Backbone deformation energy, described in detail below, accounts for structural deformation of the gramicidin helices due to thermal motion.

A group localization term is included to stabilize monomer helices during dynamics. As side chains are not included, cohesive forces involving amino acid residues are ignored. Forces between side chains may encourage stability at the monomer-monomer junction and also may help maintain the integrity of the mouth of the channel. Forces between side chains and lipid help localize the channel within the membrane. In this model, if the groups comprising the backbone are allowed to move completely freely, constrained only by the simplest backbone potential, the mouth of the channel deforms. In addition, intermonomer attraction at the junction is not of itself sufficient to allow strong dimerization interaction. While the dimer is stable (it would rather self-associate than diffuse into the aqueous domain), typically only two or three (of six possible) hydrogen bonds form. To maintain helical structure, a localization energy term is included, $\Sigma\frac{1}{2}k(r_i - r_{oi})^2$, where r_{oi} is the 0 K position of group i and $k = 5$ mdyn nm^{-1}, typical of bending deformations (Koyama and Shimanouchi, 1974); this limits group motions to the vicinity of their 0 K locations. The treatment is a compromise between Brickmann's periodic model (Polymeropoulos et al., 1985), Clementi's constrained model (Fornili et al., 1984; Kim and Clementi, 1985; Kim et al., 1985) and more general pictures (Pullman, 1987; Mackay et al., 1984; Åqvist and Warshel, 1989; Chiu et al., 1989).

TABLE 2 Lennard-Jones parameters

Groups	σ/nm	$\epsilon/kJ\ mol^{-1}$
CO-CO	0.339	0.624
CO-NH	0.341	0.534
CO-C_α	0.363	0.258
CO-Water	0.327	0.515
NH-NH	0.343	0.457
NH-C_α	0.365	0.221
NH-Water	0.329	0.441
C_α-C_α	0.388	0.107
C_α-Water	0.349	0.213
Water-Water	0.315	0.425
Cs^+-Water	0.380	0.100
Cs^+-CO	0.394	0.121
Cs^+-NH	0.397	0.104
Cs^+-C_α	0.422	0.050
Cl^--Water	0.380	0.100
Cl^--CO	0.394	0.121
Cl^--NH	0.397	0.104
Cl^--C_α	0.422	0.050

Backbone deformation

The gramicidin helix is flexible and can be deformed in a variety of ways: bond stretching, bond bending, and amide plane deformation. The free energy profile must account for these influences. Deformational forces involve group, not atom, motion. The simplest procedure is to imagine that the analogues to backbone stretching motions in gramicidin are changes in the (C_α)-(CO), (CO)-(NH), and (NH)-(C_α) distances. Similarly, bending of the C_αCN bond corresponds to (C_α)(CO)(NH) angular deformation, etc. and bending of the OCN bond corresponds to altering the angle between the orientation of the CO dipole and the (CO)(NH) bond, etc. The amide plane constraint is mimicked by assuming a restoring force whenever the dihedral angle between the planes defined by the CO dipole and the (CO)(NH) bond and by the neighboring NH dipole and the (CO)(NH) bond is not 180°. The correspondences are listed in Table 3.

The deformation potentials are:

bond stretching, $V_s = \frac{1}{2}k_s(r - r_o)^2$,

bond-bond bending, $V_b = K[1 - \cos(\theta - \theta_o)]$,

dipole-bond bending, $V_d = K[1 - \cos(\theta - \theta_o)]$, and

amide plane bending, $V_p = D(1 - n_\alpha \cdot n_\beta)$.

Here r is an intergroup separation, θ a bond-bond or dipole-bond angle, and n_α the vector defined by the normal to the plane containing the CO dipole and the (CO)(NH) bond, etc. For bond-bond bending, $\cos\theta$ is $u_{\alpha\beta} \cdot u_{\beta\gamma}$; $u_{\alpha\beta}$ is a unit vector directed from group β to group α, etc. For dipole-bond bending, $\cos\theta$ is $o_\alpha \cdot u_{\alpha\beta}$; o_α is a unit vector directed along the dipole, etc. The resultant forces (F) between the centers-of-mass of the groups are:

bond stretching, $F_\alpha = -k_s(r_{\alpha\beta} - r_o)u_{\alpha\beta} = -F_\beta$,

TABLE 3 Analogues between atom based and group based structural deformations

Deformation	Atom based	Group based
Stretch	C-N	(CO)-(NH)*
Stretch	N-C_α	(NH)-Cα
Stretch	C_α-C	C_α-(CO)
Bend	0-C-N	n_{CO}-(CO)-(NH)‡
Bend	C-N-H	(CO)-(NH)-n_{NH}
Bend	C-N-C_α	(CO)-(NH)-C_α
Bend	H-N-C_α	n_{NH}-(NH)-C_α
Bend	N-C_α-C	(NH)-C_α-(CO)
Bend	C_α-C-O	C_α-(CO)-n_{CO}
Bend	C_α-C-N	C_α-(CO)-(NH)
Amide Plane	O-C-N-H	n_{CO}-(CO)-(NH)-n_{NH}

*(CO) denotes the center-of-mass of the CO group, etc.
‡n_{CO} denotes the orientation of the CO dipole, etc.

bond-bond bending, $F_\alpha = K[\cos\theta_0 - \sin\theta_0 \cot\theta]\nabla_\alpha \cos\theta$, where $\nabla_\alpha \cos\theta = (u_{\gamma\beta} - u_{\alpha\beta}\cos\theta)/r_{\alpha\beta}$ and $F_\beta = -F_\alpha - F_\gamma$,
dipole-bond bending, $F_\alpha = K[\cos\theta_0 - \sin\theta_0 \cot\theta]\nabla_\alpha \cos\theta$,
where $\nabla_\alpha \cos\theta = (o_{\alpha\beta} - u_{\alpha\beta}\cos\theta)/r_{\alpha\beta}$ and $F_\beta = -F_\alpha$,
amide plane deformation, $F_\alpha = D\nabla_\alpha n_\alpha \cdot n_\beta$,
where $n_\alpha = (o_\alpha \times u_{\alpha\beta})/|o_\alpha \times u_{\alpha\beta}|$.
Interaction with the group dipoles creates torques (L) acting at the groups' center-of-mass; the resultant contributions are:
dipole-bond bending, $L_\alpha = -(o_\alpha \times \nabla_{o\alpha} V_d) = K[\cos\theta_0 - \sin\theta_0 \cot\theta](o_\alpha \times u_{\alpha\beta})$,
amide plane deformation, $L_\alpha = D[o_\alpha \times \{o_\beta/D_\alpha D_\beta + (\pi_\alpha o_\alpha \cdot o_\beta - \pi_\beta)u_{\alpha\beta}/D_\alpha^3 D_\beta\}]$,
where $\pi_\alpha = o_\alpha \cdot u_{\alpha\beta}$ and $D_\alpha = \sqrt{[1 - \pi_\alpha^2]}$.
The force constants are again $k_s = 20$ mdyn nm^{-1} and $K = 5 \cdot 10^{-19}$ J (Lee and Jordan, 1984; Sung and Jordan, 1987), comparable to those used in AMBER (Weiner et al., 1984). The only new parameter is D, the dihedral plane deformational energy; the value of AMBER force field, 2.5 kJ mol^{-1} is used.

Switching function

Computational time limitations require the introduction of a cut-off distance beyond which direct group-group interaction is not considered. To smooth out abrupt changes in the forces acting on the groups in the system as particles move in and out of range of one another the cut-off can be imposed gradually (van Gunsteren and Karplus, 1982). Particles are fully coupled at separations $<R_-$ and noncoupled for separations $>R_+$. For groups separated by r, the intergroup potential $v(r)$ is $f(r)v^\circ(r)$, where $f(r)$ is the, as yet unspecified, switching function and $v^\circ(r)$ is the ordinary interaction potential; $f(r)$ depends only on the distance between the particles. The modified force between an interacting pair is

$$F = -\nabla v = F^\circ f(r) - v^\circ(r)\nabla f(r),$$

where f° is the force in the absence of the cut-off. The modified torque is $L = L^\circ f(r)$ because rotation does not alter the interparticle separation; thus $f(r)$ does not change. Calculation of induced dipole moments requires knowing the electric field at location i due to charges at j. The modified expression is $E_{ij} = E^\circ_{ij} f(r)$ because in the polarization process r does not change; each contribution to the local field depends on $f(r)$, not its gradient.

The choice of switching function is, within limits, quite arbitrary. Defining the variable $x \equiv (r - [R_+ + R_-]/2)/[(R_+ - R_-)/2]$, the necessary constraints on $f(x)$ are

$$f(-1) = 1, (r = R_-, \textit{full coupling})$$
$$f(1) = 0, (r = R_+, \text{no coupling}).$$

$f(x)$ is assumed symmetric about the midpoint of the cut-off region and gradually increments the force between interacting pairs; consequently, $f(0) \equiv 0.5, f'(-1) \equiv 0$, $f'(1) \equiv 0$. The simplest function satisfying these conditions is

$$f(x) = 0.5 + 0.25x(x^2 - 3).$$

Simulational details

As the ion is translated through the channel, umbrella sampling is used to link neighboring regions (Pangali et al., 1979). In this process, the ion is constrained to the vicinity of the plane $z = z_w$ (a window) by means of an harmonic restoring potential, $V_w = \frac{1}{2}k_w(z - z_w)^2$. Upon completion of a calculation for one window the ion is translated to its next location in the channel and the process repeated; windows are separated by from 0.5–1.0 Å, depending on the rapidity with which the potential changes.

The cut-off and switching procedure outlined above was used; particles are fully interacting at 7.5 Å and out of range at 8.5 Å. Temperature control is maintained by Langevin coupling with a relaxation time of 0.1 ps (Berendsen et al., 1985). A 5-point predictor corrector is used to solve the equations of motion (Gear, 1971). Rotational coordinates are described by Cayley-Klein parameters (Evans and Murad, 1977). Moments of inertia are increased: for the polar groups of the helix 10-fold and for water 100-fold (in some early calculations, the latter only 10-fold). The mass of Cs^+ is decreased by a factor of 2. The effect is to slow down the rate of water, carbonyl, and NH rotation and to slightly speed up the translation of the ion. In this way both rotational and

translational energy transfer are facilitated and phase space sampling made more efficient. As equilibrium properties are determined by the interaction potential alone, such artifices have no thermodynamic consequences (McQuarrie, 1976).[4] This permits relatively large time steps to be used in the calculation, reducing the amount of computer time required; 2 fs steps are adequate. A similar device (increasing the mass of H atoms for more efficient configurational sampling at larger time steps, in this case 4 fs) has been used in theoretical studies of relative binding affinities (Lybrand et al., 1986).

In each window the system is re-equilibrated for at least 8 ps and data are collected for 25–40 ps. The potential of mean force (PMF) at z, $w(z)$, describes the free energy profile for ion permeation. It is simply related to the probability, $\rho(z)$, of finding the ion at that location, corrected for the window potential (McQuarrie, 1976; Pangali et al., 1979),

$$w(z) = -kT \ln \rho(z) + V_w(z) + C_w;$$

$\rho(z)$ is determined by counting how often the ion is found in a particular region (bin) near z and the bins are 0.1 Å in width. As the constant C_w varies from window to window, neighboring windows must be overlapped by matching the slope of the local PMF to continue the construction of the potential. Overlap involved from 3 to 10 "significant" bins; the average number was 5. The mean uncertainty in overlapping the PMF was $\leq \pm 2.0$ kJ mol^{-1}, usually $\leq \pm 1.0$ kJ mol^{-1}. Because of the number of windows required (22), error accumulation is inevitable. If overlap errors are randomly distributed, the total uncertainty in relative energy in the PMF between the 14.0 and 0.0 Å regions is $\approx \pm 5$ kJ mol^{-1}. In more limited regions the uncertainties introduced by overlap errors are less, e.g., between mouth and peak (14.0 and 9.7 Å), the random error is ± 2.6 kJ mol^{-1}, a small fraction of the total energy change. Umbrella sampling was not continued beyond 14.3 Å; in these regions the ion is no longer constrained by the channel geometry and accurate dynamical sampling requires far more extended periods of data collection than 40 ps.

RESULTS

The computations provide significant data related to ion-water and ion-polypeptide correlation. In addition to discussing the PMF for Cs^+ permeation, selected results related to helix structure, water-water correlation, ion-water correlation, ion-carbonyl correlation, and water-carbonyl correlation, are described. The systems of interest are the ion-free channel, Cs^+ at selected locations in the channel and Cl^- in the channel mouth. Of special interest is how the local environment affects properties of water; how the ion perturbs the gramicidin helix; what interactions most significantly influence water-water correlation; how the pore environment affects ionic solvation and coordination; and how to identify the single-file region.

Helix structure

The model is unusual because the basic dynamical unit is a polarizable dipolar group, not an atom and so charge separation between atoms in the groups is not incorporated. The thermalized, water-filled helix differs structurally in only a few respects from the model which provided the starting point for the analysis. The mean OCN angle[5] decreases by 3.5°, presumably due to the strong electrostatic interaction of carbonyl groups and water molecules. Standard deviations in bond angles range from 4 to 8°; the most variable is the $NC_\alpha C$ angle, as at the C_α linkage the peptide plane constraints have the least restraining influence. The deformational energies associated with a one standard deviation angular displacement are between 0.75 and 3.0 kJ mol^{-1} (0.3–1.2 k_BT). Only two individual bond angles stand out as strikingly different from the average for a specific bond angle type. The CNC_α angle at the amino terminus (the dimer junction) exhibits an unusually large standard deviation, typically 1.5 times the average; the $NC_\alpha C$ angle at the ethanolamine tail is exceptionally variable, with a standard deviation of ± 14°, nearly twice the average for that bond type. Even though no other bond angles at either the junction or the tail are unambiguously different from those in the remainder of the helix, the dimer junction and the ethanolamine tail are clearly regions of extra structural flexibility. The same general observations hold if an ion is in the channel.

Potential of mean force

Depending upon the ion, single channel conductance data suggest entrance and/or translocation barriers no greater than $\approx$20–40 kJ mol^{-1} (Hladky and Haydon, 1972; Bamberg and Läuger, 1974; Andersen and Procopio, 1980; Urban et al., 1980; Urry et al., 1980; Eisenman and Sandblom, 1983). The inference drawn from some analyses is that the ion is more stable in the channel environment than in bulk solution (Jakobsson and Chiu, 1987;

[4]A study of the properties of monovalent ion-water microclusters (Lin and Jordan, 1988) provides a few examples that such rescaling has no effect on equilibrium behavior.

[5]Reference is to bond angles, not the analog deformations listed in Table III.

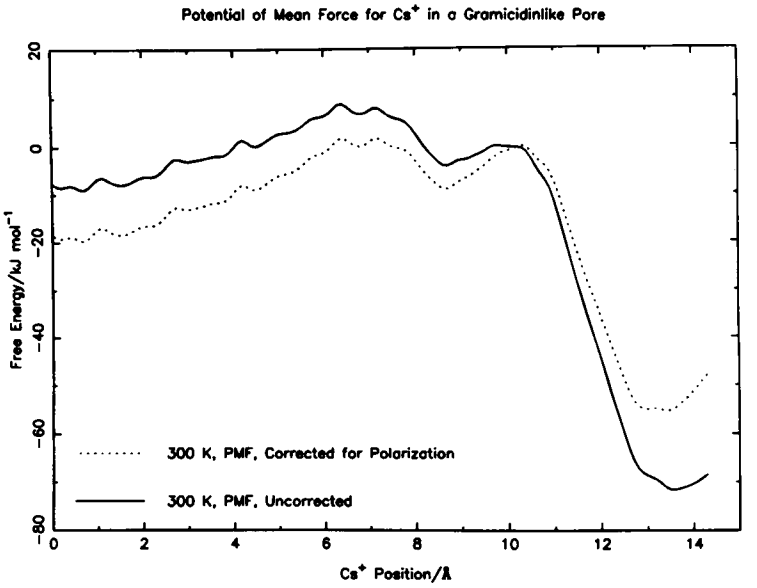

FIGURE 1 Potential of mean force (PMF) for Cs^+ and PMF, adjusted for polarization corrections, as described in text. In determining the polarization energy correction, the lipid is assumed to have a dielectric constant of 3, the gramicidin backbone a radius of 5 Å, and the channl a length of 25 Å. Profiles are adjusted so that the energy at the peak of the entrance barrier is zero. Distances are measured from the midpoint of the pore; the potential profile should be symmetric about the midpoint.

Chiu and Jakobsson, 1989). Fig. 1 presents the PMF constructed using umbrella sampling.[6] There is a binding site in the channel mouth, ~13.5 Å from the channel midpoint, where the ion maintains most of its aqeuous hydration shell and also interacts strongly with the #11 CO of the channel. Whereas the free energy varies relatively little once the ion has entered the channel interior, there is a clearly articulated secondary minimum near 9.0 Å. Beyond the global maximum near 6.5 Å, the free energy drops gradually as the ion approaches the dimer junction. The energy barriers to translocation, ≈70 kJ mol^{-1} for ion entry from the minimum into the single file region and ≈80 kJ mol^{-1} for passage over the global maximum near 6.5 Å, are too large.

While well defined, the physical system is a highly approximate representation of gramicidin. The amino acid side chains are ignored even though substituting the tryptophans by less polar residues is known to lower channel conductance (Bamberg et al., 1976; Heitz et al., 1982; Mazet et al., 1984; Koeppe et al., 1988). Replacing all tryptophans by phenylalanines reduces the single channel conductance (Heitz et al., 1982, 1984) by ~25-fold at low voltages, equivalent to raising the entrance barrier ≈8 kJ mol^{-1}. The effect in a polyglycine analogue should be substantially larger. The membrane has been incorporated in a rudimentary fashion. The actual lipid is ≈100–200 mV positive with respect to water (Paltauf et al., 1971; Hladky and Haydon, 1973; Pickar and Benz, 1978). While dielectric shielding reduces the potential in the channel interior by ≈60% (Bamberg et al., 1976; Jordan, 1983) there is still an associated energy barrier ≈10 kJ mol^{-1}. Additionally, this treatment of the lipid does not account for its electrostatic influence on water, channel, or ion. Finally, the use of the 8 Å cut-off, needed to reduce calculational time, introduces further uncertainty because the composition of the excluded regions changes markedly as the ion moves from water into the channel.

The electrostatic influence of the lipid on the potential profile can be accounted for. As modeled, the lipid, a region of dielectric constant $\epsilon \approx 2$–3, is treated as one with $\epsilon = 1$, i.e., an electrical vacuum. The missing terms are attractive and lower the free energy. The stabilization energy can be estimated using continuum electrostatic modeling methods (Jordan, 1981, 1984) as the energy recovered by modifying the "lipid-like" domain so that it has an ϵ of 2–3. Because this stabilization energy varies little as an ion moves off axis (Vayl and Jordan, 1987) it can be computed by describing the "lipid" as an annulus with interior radius 5 Å (the radius of the gramicidin backbone), infinite exterior radius and height 25 Å embedded in a dielective vacuum. The stabilization energy is the decrease in ionic polarization energy as the

[6]Some features of this PMF have been described in a preliminary communication [Jordan, 1988].

dielectric constant of the annulus is varied from 1 to 3. The total polarization energy for ion translocation from bulk water to the channel midpoint is ≈ -60 kJ mol^{-1}. Correcting the PMF yields the dotted curve shown in Fig. 1 (the full 60 kJ mol^{-1} stabilization is not visible because $\approx$70% of the energy change occurs between 13.5 Å and the bulk). The minimum near 13.5 Å is deeper. The entrance barrier is reduced to $\approx$55 kJ mol^{-1} and the absolute maximum, $\approx$7.0 Å from the midpoint, is also $\approx$55 kJ mol^{-1}.

The differential effect of the 8 Å cut-off, due to the change in composition of the excluded regions as the ion moves from water into the channel, has been estimated qualitatively (Jordan, 1988). The cut-off errors vary significantly from region to region. The largest corrections occur for an ion near the peak of the entrance barrier (≈ -60 kJ mol^{-1}), the smallest for one in the channel mouth (≈ -30 kJ mol^{-1}), and intermediate corrections throughout the channel interior (≈ -50 kJ mol^{-1}). In the single file region of the channel, the structure of the PMF does not change significantly. The cut-off affects the energy most noticeably in the region near 10 Å. The entrance barrier from bulk water is reduced sharply and the exit barrier from the single file region is raised slightly.

Helix dipoles

The mean dipole moments of the CO, NH, and C_α groups are 2.56, 1.08, and 0.15 Debye, respectively, much larger than their uncompensated values, 2.26, 0.86, and 0.00 Debye; they do not change notably if an ion is in the channel. For CO and NH, the averages are less than those computed previously, 2.65 and 1.30 Debye, respectively (Sung and Jordan, 1987), which were typical of the peptide backbone (Pethig, 1979). In the earlier work second neighbors were allowed to interact; here neither first nor second neighbor dipolar groups of the backbone interact electrostatically. The reduction in polarization interaction indicates that explicit neglect of charge separation is not without consequences.

Dipole moments of individual groups show significant variation. For the ion-free channel, average dipole moments in the helix interior differ little from one another or from the mean. Behavior at the channel mouth is much different. As a direct result of polarization, the endo-CO's (10, 12, and 14 in each helix) have abnormally low dipole moments, averaging $\approx$2.51 Debye, while the exo-CO's (11, 13, and 15 in each helix) are unusually high, averaging $\approx$2.67 Debye. Analogous alternation is observed for the complementary NH's; the endo-groups (11, 13, and 15) are high (mean $\approx$ 1.16 Debye) whereas the exo-groups (10, 12, and 14) are low (mean $\approx$ 1.02 Debye).

TABLE 4 Mean dipole moments, μ, for water in different environments

Environment	μ/Debye
Bulk	2.47 ± 0.05
Bulk, waters neighboring Cs^+	2.47 ± 0.05
Channel, no ion present	2.31 ± 0.03
Channel, waters not neighboring Cs^+	2.35 ± 0.02
Channel, waters neighboring Cs^+	2.52 ± 0.10

Water dipoles

Including polarizability also has a marked effect on water's properties. Within the channel, water cannot form the hydrogen-bonded network structure typical of bulk water which greatly alters its mean dipole moment, $\langle\mu\rangle$. Table 4 lists $\langle\mu\rangle$ for water in its different possible environments. A number of points are evident. Pore water differs strikingly from bulk water. The $\langle\mu\rangle$'s are sharply reduced from their bulk averaged values ($\approx$2.47 Debye, in essential agreement with previous calculations using the same model [Barnes et al., 1979]). With Cs^+ in the pore the $\langle\mu\rangle$'s of its neighboring waters are high; those of the remaining pore water molecules are relatively small (but slightly larger than in the ion-free case). The $\langle\mu\rangle$'s for channel waters neighboring Cs^+ are equal to those of water in $Cs(H_2O)_2^+$ microclusters (Lin and Jordan, 1988); additionally, mean Cs^+-water separations are the same in the dihydro-microcluster as in the analogously hydrated channel milieu. In bulk, water molecules neighboring Cs^+ exhibit $\langle\mu\rangle$'s not much different from those found for water itself.

Single filing and pore occupancy

Our calculations suggest two different natural ways to identify the number of water molecules within the pore. At 300 K, channel waters cannot overtake one another; only in the mouths of the channel can there be water interchange. Consistent with previous studies (Mackay et al., 1984; Skerra and Brickmann, 1987*a*, *b*; Chiu et al., 1989), in 34 ps of dynamics for an ion-free channel,[7] illustrated in Fig. 2 *a*, a file of nine axially located water molecules appears to move like a rigid body, almost as if it were a single massive particle.

[7]It should be noted that the dynamics only serves to illustrate the nature of the ion-water and water-water correlations; the actual time scale of the events must be different for three reasons. Langevin coupling (Berendsen et al., 1985) is used to mimic canonical coupling; second, the Cs^+ has had its mass reduced by a factor of two; third, the groups have artificially increased moments of inertia (the water molecules 100-fold and the polar groups of the helix 10-fold).

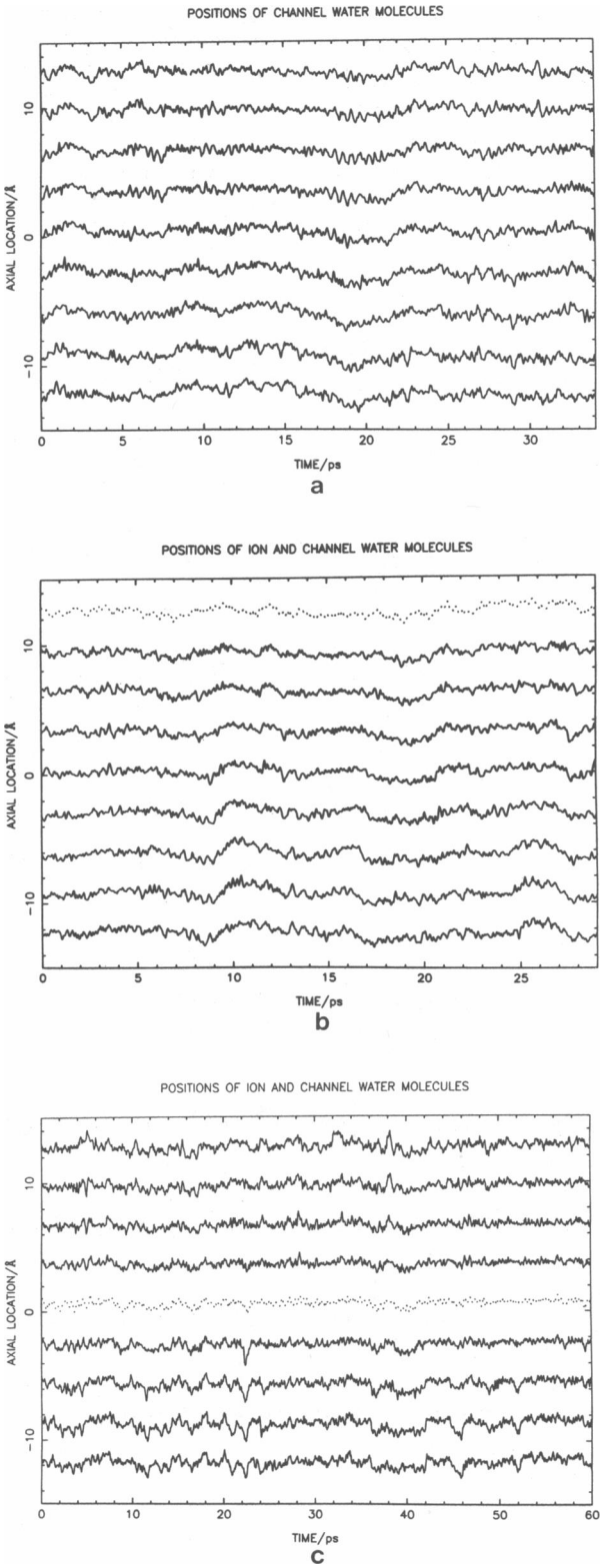

FIGURE 2 Dynamics of channel water molecules and ion at 300 K for three cases: (*a*) ion-free channel; (*b*) Cl^- near 12.5 Å; (*c*) Cs^+ near 0.5 Å (designations are mean distances from dimer junction). The solid traces represent water locations; the dotted traces represent the ions. In all instances illustrated there are nine groups in the single file.

The motion of water molecules in the no pass region is highly correlated. As seen in Fig. 2, regardless of whether an ion is present, where it is located, or its charge, the whole file behaves like a single rigid body. All particles attain their maximum (or minimum) axial location at essentially the same instant. Separation between neighboring groups is roughly constant. Fig. 3 *a* illustrates this differently by presenting the distance between complementary water molecules in an ion-free channel, i.e., those a distance $\approx \pm L$ Å from the channel midpoint. The separations do not change markedly; only when two water molecules are separated by just one interstitial water do the fluctuations differ. Even the waters in the channel mouth (at ± 12 Å) are closely coupled to the waters in the file and exhibit (at least on the time scale illustrated) no tendency to exchange with bulk water. Fig. 3 *b* presents similar information for Cs^+ near the dimer junction (≈ 0.5 Å); the observations with respect to water correlation are

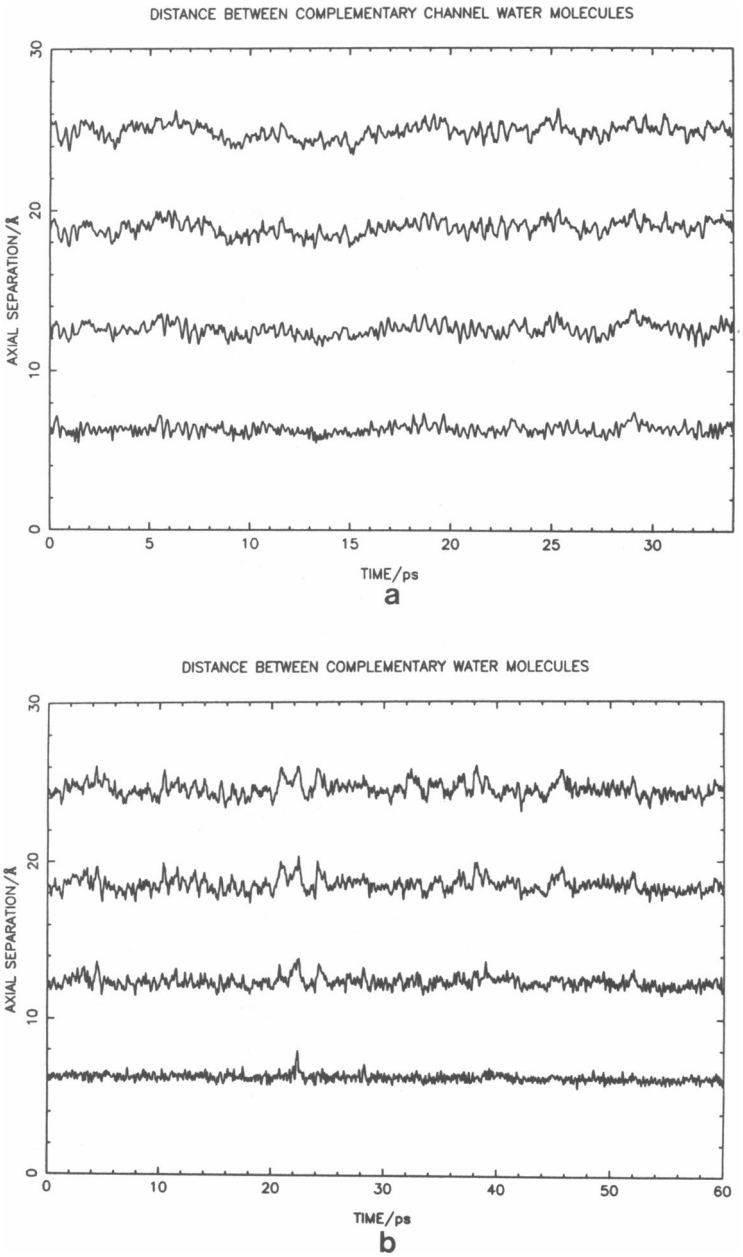

FIGURE 3 Distance between complementary (those $\pm L$ Å apart) water molecules demonstrating the high degree of translational correlation in (*a*) an ion-free channel, (*b*) channel with Cs^+ near the dimer junction (≈ 0.5 Å from midpoint).

identical. The ion, as seen by comparison with Fig. 3 *a*, encourages more correlated water motions than when the channel is ion-free. The fluctuations in the axial distances between waters spanned by both ion and water are clearly smaller than when no ion is present. This is most apparent in the comparison of the 6 Å traces; however, it is noticeable for all of them.

Water-water and ion-water orientational correlations

There are no persistent orientational correlations propagating the length of the channel such as those observed by Mackay et al. (1984) and Chiu et al. (1989). Rather, in the absence of an ion, water-water angular correlation at the termini is controlled by the carbonyl groups in the channel mouth. With an ion present, it naturally dominates. The mouth structure propagates, but does not extend to the channel's other side. Fig. 4 presents three snapshots of the water in the single file region, with and without an ion present. In no case does dipolar orientation persist.

These points are emphasized in Fig. 5 which presents the axial component of the normalized water dipole vector (n_z) for channel waters. Data were collected at 0.25 ps intervals. The labeling along the right-hand axis indicates each water's approximate axial location. Positive n_z's indicate that the oxygen end of the water dipole is oriented in the $+z$ direction (toward the channel's right-hand mouth). Five cases, which illustrate the influence of valence or effects in different dynamical regions, are depicted: (*a*) no ion present; (*b*) Cs^+ near the exterior minimum in the PMF, $\approx +13.7$ Å, where it is still substantially hydrated; (*c*) Cl^- near $+12.5$ Å; (*d*) Cs^+ just inside the entrance barrier, $\approx +9.5$ Å, where it has only two waters of hydration; (*e*) Cs^+ near the dimer junction, $\approx +0.5$ Å.[8] In each instance the top trace (water in the channel's left-hand mouth) indicates that n_z is generally positive, i.e., a water's hydrogen atoms are pointed outward (as in Fig. 4) and are associated with the carbonyl groups which form the channel mouth; the oxygen is inside the channel. Except for case *b* the bottom trace (water in the channel's right-hand mouth) exhibits opposite water orientation. In cases *a* and *e* this water is again aligned by the carbonyl groups of the mouth. When Cl^- is in the channel mouth, case *c*, or when Cs^+ is near the peak of the entrance barrier, case *d*, the carbonyl groups and the ion cooperate in orienting the water dipole. Only when Cs^+ is located just outside the mouth, case *b*, is this water dipole reversed.

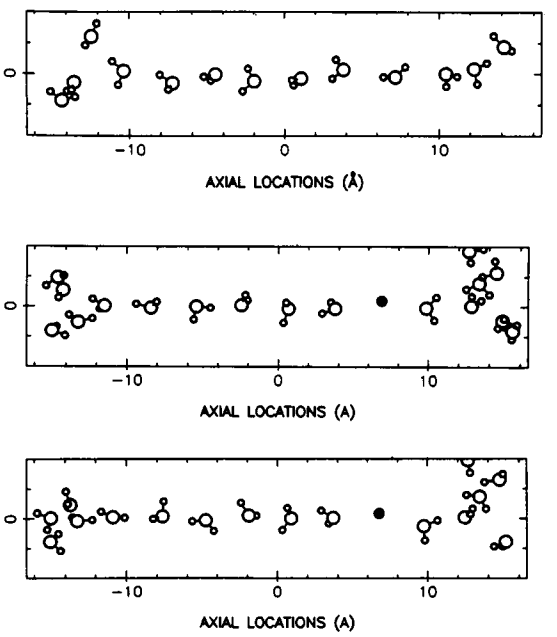

FIGURE 4 Water alignment at 300 K within the channel for (*top*) ion-free channel; (*middle*) and (*bottom*) Cs^+ near 8.4 Å from the channel midpoint. The ions are depicted as solid circles. The projections emphasize the nature of the water alignment. Dipolar alignment does not extend across the channel. (Reprinted by permission from [Jordan, 1987]; copyright 1987, American Chemical Society.)

Ion-helix correlation

The presence of an ion in the channel has little effect on the backbone structure. It significantly influences the axial orientation of the dipoles. In an ion-free channel, water molecules attract both sets of polar groups. They create a slight tendency, shown in Table 5, for both NH and CO groups to tilt toward the channel axis. With Cs^+ in the channel there is strong cation-oxygen attraction and cation-hydrogen repulsion; the mean tilt is somewhat dependent on ion location. Consequently the CO's bend in and the NH's tilt out. With Cl^- as the ion, the effect is reversed.

The effect of ion-group (or water-group) interaction is most clearly apparent in the orientation of groups close to the ion (or water). Fig. 6 *a* illustrates the angular deflections of the CO groups for an ion-free helix. There is a general pattern of alternation. With Cs^+ present the

[8]Differences in fluctuation frequency reflect changes in the scaling of water's moments of inertia. For the higher frequency oscillations moments have been increased 10-fold and for the lower frequencies, 100-fold. As indicated in footnote 4, the artifice has no effect on equilibrium properties (McQuarrie, 1976). It should again be stressed that the dynamics only illustrates how reorientation occurs while the time scale has no precise significance.

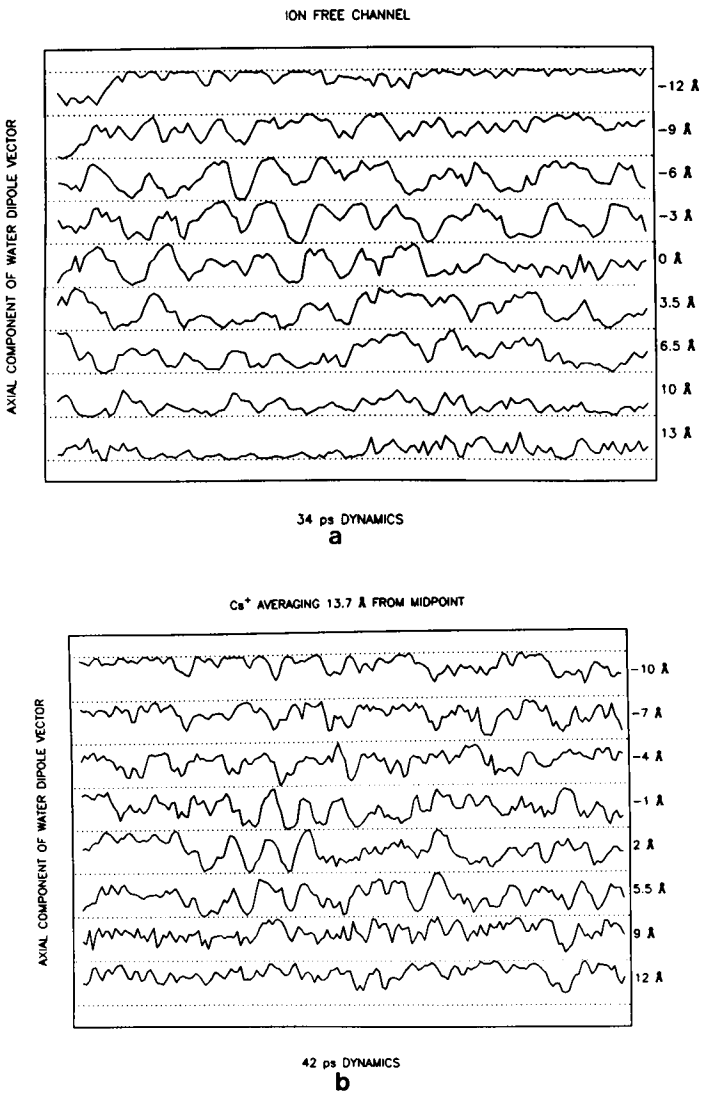

FIGURE 5 Dynamics of dipolar alignment of channel water molecules at 300 K for selected configurations: (*a*) ion-free channel; (*b*) Cs^+ near 13.7 Å; (*c*) Cl^- near 12.5 Å; (*d*) Cs^+ near 9.5 Å; (*e*) Cs^+ near 0.5 Å (locations are mean distances from the dimer junction). The labels along the right-hand axis indicate the approximate axial location of the water molecules. A positive deflection indicates that the oxygen atom of the water dipole is directed toward the right-hand mouth of the channel (the $+z$ direction). In cases *b* and *c*, the ion is external to the file of water; in case *d* it is between the last two waters; in case *e* it is in the middle. Only in case *e* are all water molecules in the channel interior obviously aligned; in all other examples, with the possible exception of case *d*, there is no clearly preferred orientation for water molecules within the channel. In cases *a*, *c*, and *d* water moments of inertia have been increased to 100 times their actual values; in case *b* the factor is only 10; in case *e* the factor is 10 for the first 30 ps (rapid fluctuation) and 100 thereafter. The dotted lines are $\boldsymbol{n}$ values for which $\boldsymbol{n} \cdot \boldsymbol{k} = \pm 1$, i.e, perfect axial alignment.

pattern is different. For the ion near the channel center, Fig. 6 *b* presents the *differential* deflection of the CO groups (the difference between a CO group's mean angular deflection in an occupied channel and the corresponding quantity in an ion-free channel). In magnitude, the maximum difference is ≈40°. Fig. 6 *c* depicts similar results with Cs^+ just inside the entrance barrier (≈9.5 Å). The maximum difference here is ≈30°.

Fig. 7 illustrates orientational correlation between the ion and its nearest neighbor polar groups by plots of $\boldsymbol{n} \cdot \boldsymbol{u}_{i \to g}$, where $\boldsymbol{n}$ is a unit vector along the dipolar axis and $\boldsymbol{u}_{i \to g}$ is a unit vector directed from the ion to the center-of-mass of the polar group. For carbonyl-cation interaction, perfect alignment occurs for $\boldsymbol{n} \cdot \boldsymbol{u}_{i \to g} = +1$, etc. The configurations are the ones described in Fig. 5: (*a*) Cs^+ near 13.7 Å; (*b*) Cs^+ near 9.5 Å; (*c*) Cs^+ near 0.5 Å; (*d*) Cl^- near 12.5 Å. With Cs^+ in the channel mouth (Fig. 7 *a*), the ion almost locks on to CO #11; alignment is

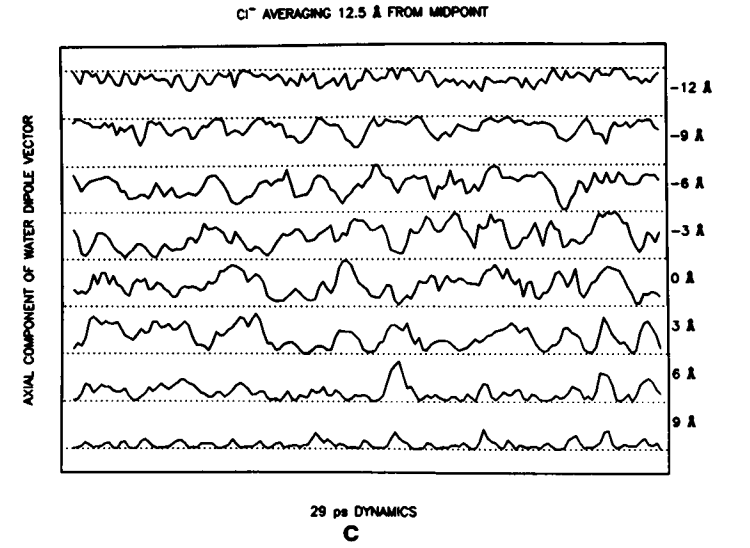

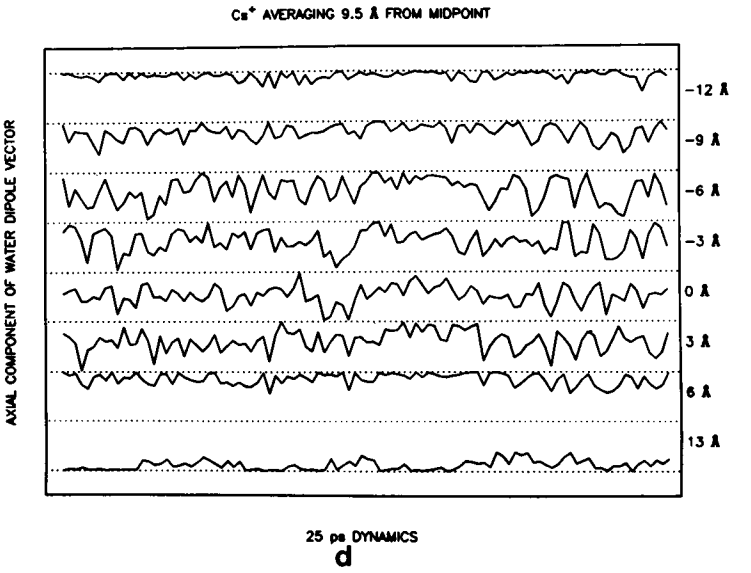

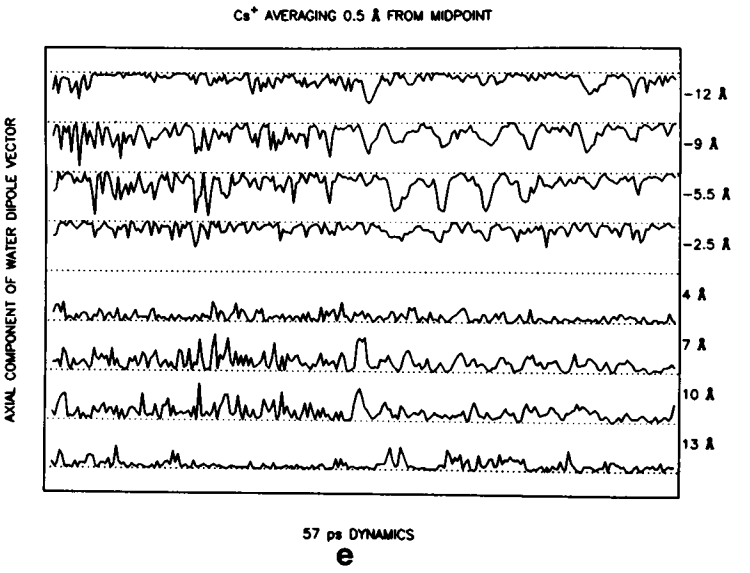

FIGURE 5 (continued)

TABLE 5 **Mean deflection angles of polar groups as function of channel occupancy**

Group	Water occupancy	Cation occupancy	Anion occupancy
CO	−0.5°	−4° to −6°*	+2°
NH	−1.5°	3° to 4°	−3°

*A range is indicated because mean angular deflection varies with cation location in the channel; no similar range is noted for anion occupancy because in all configurations studied the anion was in the channel mouth.

nearly perfect. In all instances the ion and its nearby carbonyl groups are strongly correlated; for NH the effects are weaker, reflecting their smaller dipole moments. In case *d*, Cl^-, the orientation pattern is naturally reversed and the correlations appear to be somewhat weakened. Cases *a*, *b*, and *d*, with an ion close to the channel mouth, illustrate the relatively weak direct interaction with COH of the ethanolamine residue; this is indicated by sporadic misalignments, i.e., $\boldsymbol{n} \cdot \boldsymbol{u}_{i \to g}$ is occasionally <0 for Cs^+ and >0 for Cl^-. It also demonstrates clearly the flexibility of the ethanolamine tail region, a point first emphasized by Etchebest and Pullman (1984).

Ion coordination

In moving from bulk to the single file region of the channel, the ion undergoes significant solvation changes. In bulk, Cs^+ is essentially hexacoordinate. As it enters the channel mouth, the pattern changes; it loses many of its waters of hydration and binds to carbonyl groups. The coordination pattern in the channel is summarized in Table 6. The coordination condition is Cs^+-oxygen distance ≤ 3.5 Å; increasing this to 3.7 Å has no effect on the conclusions. In the channel mouth (the region near 13.7 Å), Cs^+ is hexacoordinate, 5.0 water molecules and 0.9 CO's. As it enters the channel this changes. It remains hexacoordinate through much of the entry process as it sheds waters of hydration and becomes liganded to more carbonyls. There is an abrupt change in the region between 11.3 and 9.5 Å from the midpoint. It enters an interior single file and it gradually becomes pentacoordinate. It binds two water molecules and a specific pair of carbonyls (with mean ion-oxygen distance ≤ 3.3 Å); in addition it shuttles among three others so that it always has about five ligands.[9] This continues until it approaches the midpoint. Here coordination changes again; it becomes nearly hexacoordinate, binding with 3.8 carbonyls in addition to its two single file waters.

[9]Shuttling is in part due to impositing windowing potentials that constrain the ion to limited regions of the channel. It is possible that if the window constraint were released the ion could associate somewhat more strongly with a third CO and less strongly with the other two of the triad. There would be no change in net coordination number.

DISCUSSION

Many of the results described in the previous section are similar to those found by previous investigators, even though the models are very different. In a few instances the present calculations yield notably dissimilar predictions. When the conclusions based on the various models are in general agreement it suggests that they are most likely reliable guides to the behavior of gramicidin itself. On the other hand, when the conclusions diverge, the reason is to be found in the differences between the potential functions and there is no certain basis for deciding which model more closely describes gramicidin. I will critique the model, discuss some of its more significant consequences and then compare its predictions to those of previous studies.

The model

The approach differs significantly from that taken by others. The influence of polarization of the polar groups by the ion is treated explicitly. This has the advantage that the charge distribution of groups near an ion can be perturbed by the ion; their properties can (and do) differ substantially from the group average. There is, however, a price. The model parameters are less well optimized than those used in more standard force fields (GROMOS, AMBER, CHARMM). Furthermore, the basic units are dipolar groups (CO and NH), not charged atoms (C, O, N, and H). Consequently orientational alignments due to steric influences may not be handled as well. The Lennard-Jones potentials for the polar groups are single spheres centered at the group center-of-mass. For NH this is little different from a 6-12 potential centered on N; for CO it is quite different from a pair of 6-12 potentials, centered on the C and the O. Additionally, the charges in the polar groups are not separated, but treated as point dipoles. However, as the mean helix structure in the thermalized system does not differ greatly from that of the 0 K configuration, it would seem that the model incorporates the essential features of the gramicidin helix.

Potential of mean force

Cations partition easily into the channel. Experiment suggests that the free energy barrier to ion entry is low

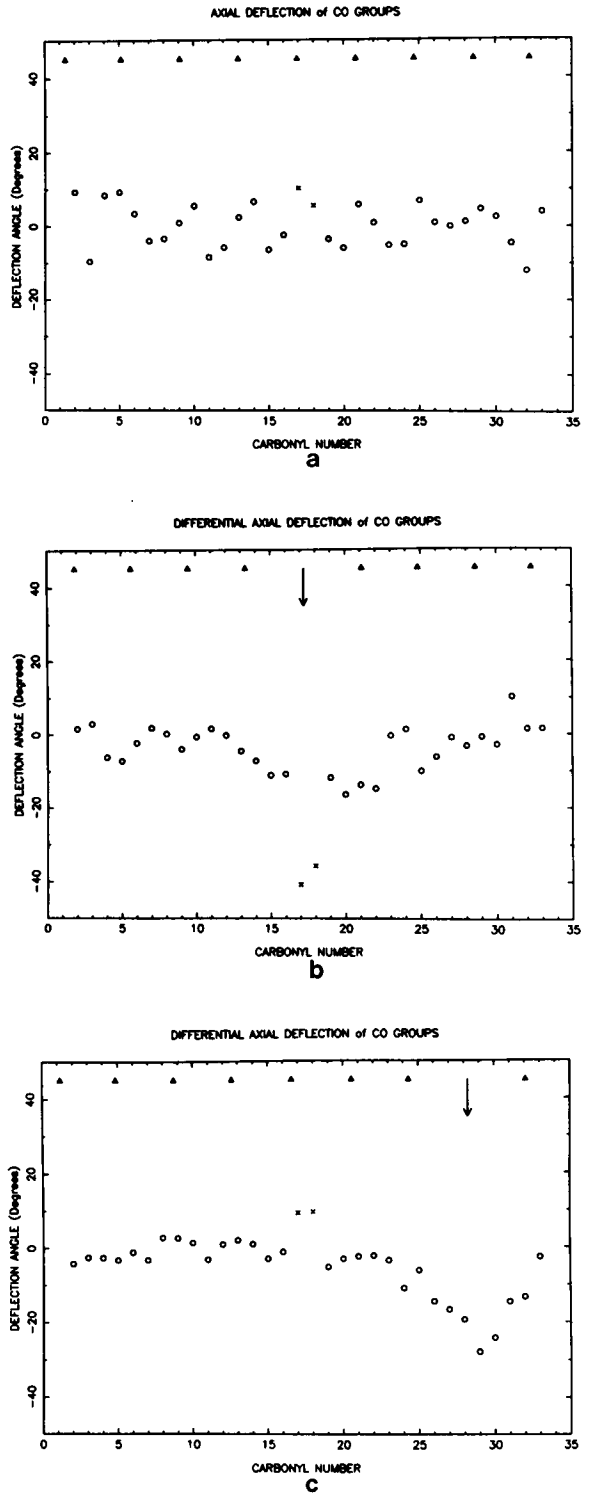

FIGURE 6 Axial angular deflections of carbonyl groups for (*a*) an ion-free channel. *Differential* angular deflections (see text) of carbonyl groups for (*b*) Cs^+ near 0.5 Å (the dimer junction), and (*c*) Cs^+ near 9.5 Å (the peak of the entrance barrier). Formyl carbonyls are denoted by (*x*); approximate water locations are indiated by (Δ); the arrow denotes approximate ion location. Negative deflections denote inward tilt. Groups have been renumbered so that the carbonyl in the left-hand mouth is 1 and that in the right-hand mouth is 32; the correspondence with the standard numbering is CO-15′ is 1, CO-0′ is 16, CO-0 is 17, CO-15 is 32, etc.

TABLE 6 **Local solvation structures in various regions of the channel**

$\langle z \rangle$/Å	# of Waters	# of CO's	CO's bound to ion*	CO's near ion‡
0.5 ± 0.2	1.9	3.8	0′, 2′, 2, 4	0
1.5 ± 0.3	2.0	2.8	0′, 4	2′, 1, 2, 6
2.5 ± 0.4	2.0	3.4	1, 6	0′, 4
3.6 ± 0.3	2.0	3.4	1, 6, 8	3, 4
4.7 ± 0.3	1.9	2.8	3, 8	5, 6, 10
5.6 ± 0.3	1.9	3.3	5, 10	3, 8
6.6 ± 0.4	2.0	3.3	5, 10	7, 8, 12
8.1 ± 0.3	1.9	3.4	7, 12	9, 10, 14
8.9 ± 0.2	2.0	3.0	9, 14	7, 11, 12
9.5 ± 0.2	2.0	3.0	9, 14	11, 12, 16
10.0 ± 0.2	2.1	3.4	14, 16	9, 11, 12
10.7 ± 0.4	2.5	2.8	11, 16	9, 13, 14
11.3 ± 0.3	3.6	2.4	11, 16	13
11.7 ± 0.2	3.7	2.4	11, 16	13
12.3 ± 0.2	4.0	2.1	11	13, 16
12.7 ± 0.1	4.6	1.7	11	16
13.7 ± 0.3	5.0	0.9	11	

*Ion-O separation averaging ≤ 3.3 Å.
‡Ion-O separation averaging > 3.3 Å and ≤ 4.0 Å.

and even, according to some interpretations, that the cation is more stable in the channel interior than in bulk solution (Jakobsson and Chiu, 1987; Chiu and Jakobsson, 1989). The free energy calculations exhibit far too high an energy barrier. This indicates the limits of the calculations, both as to the potentials employed and to the physical simplifications introduced. Charge separation in the channel interior is not adequately treated; ion-oxygen interaction in particular may be notably more stabilizing than is describable by a dipolar model.

Because of the model and computational limitations outlined in the description of results, the PMF of Fig. 1 is an uncertain guide to permeation energetics through real gramicidins. Its major simplifications are to neglect the influence of phosphatidyl head groups and polar amino acid side chains and to use an 8 Å cut-off which has very different consequences in different parts of the channel. It is thus least accurate in accounting for the energy of resolvation during ion entry into the channel and should be most reliable in describing the channel's single file region.

The computed energy barriers to Cs^+ translocation through the model channel (Fig. 1), ≈70 kJ mol^{-1} for entry from the minimum into the single file region and ≈80 kJ mol^{-1} for passage over the global maximum near 6.5 Å, are large. Direct comparison with estimated entrance barriers for real gramicidins is not possible because considerable free energy change may occur as the ion approaches the channel mouth. As indicated in Methods, umbrella sampling further from the channel mouth is impractical because in this region the ion is only weakly constrained by channel geometry and reliable dynamical sampling requires exceedingly long runs. While lower than analogous barriers found in earlier fully microscopic calculations that attempt to incorporate bulk water, e.g., Na^+ (100 and 120 kJ mol^{-1}, entrance and global), K^+ (115 and 120 kJ mol^{-1}, entrance and global) (Kim and Clementi, 1985), and for Cs^+ (170 kJ mol^{-1}, global) (Mackay, D. H. J., P. M. Edelstein, and K. R. Wilson, unpublished results), the predictions do not agree with the upper bound of 20–40 kJ mol^{-1} expected from experiment. Other studies, which treat only a few water molecules (Etchebest and Pullman, 1986; Sung and Jordan, 1987), are not truly comparable.

Only Åqvist and Warshel's (1989) cation permeation free energy profile has yielded reasonable results for both entrance and translocation barriers, ≈20 kJ mol^{-1}. Na^+, its two nearest water neighbors and the gramicidin helix (including side chains) are treated microscopically; the remainder of the system (water as well as membrane) is described by a mean field theory, the Protein-Dipole-Langevin-Dipole (PDLD) approach (Warshel and Russell, 1984). This incorporates the distinctly different long-range influences of membrane and water on the ion at different channel locations into the treatment. However, even here the ion is less stable in the channel interior than in bulk water.

Comparison of Åqvist and Warshel's (1989) profile with Fig. 1 indicates that, as the present calculations are completely thermalized, smoothing out local structure in the potential profile, energy variation is more gradual. But for one feature, the profiles are topologically similar. After the main entrance barrier, the free energy drops,

rises to the global maximum and decreases to a minimum when the ion is near the dimer junction. The striking qualitative contrast is their observation of two sharp minima near the mouth, not seen here. This could be an artifact of their mean field treatment. After determining the energy minimized structure of an ion-water-gramicidin ensemble containing 20 waters, they treat only two waters explicitly in implementing the PDLD method; the remaining waters are approximated by Langevin dipoles. This is problematical near the channel mouth where the ion's hydration number changes rapidly and where more than two waters are directly solvated by the cation.

Even though the translocation barrier ($\approx$55 kJ mol^{-1}, corrected for lipid polarization) is about double theirs, in both calculations the free energy near the dimer junction is $\approx$10 kJ mol^{-1} lower than at the minimum just inside the entrance barrier. The global maximum is 6–7 Å from the dimer junction, somewhat further out than their calculation which places it at 5.8 Å. This may reflect model differences or the differences between Cs^+ and Na^+. Here, the primary entrance barrier is located near 10.5 Å whereas theirs is at 11.5 Å. The reason for the discrepancy is unclear but it could be related to their including only two explicit waters in the energy analysis; at 11.5 Å we find that Cs^+ still directly coordinates ~3.5 waters.

Helix dipoles

At the channel mouth there is a striking pattern of alternation among the CO and NH dipole moments, reflecting the importance of polarization. These are due to water's influence on the charge redistribution in the carbonyl groups. The large induced dipoles of the exo-carbonyl groups arise because of the axially asymmetric electrostatic environment at the helix mouth; these CO's interact directly and at short range with hydrogen atoms of both bulk and channel water and are more effectively polarized than the interior carbonyls. All exo-carbonyls exhibit net dipolar attraction to the nearby water molecules, encouraging further polarization. The strongest dipole-dipole interactions within gramicidin are among sets of neighboring CO groups and among sets of neighboring NH groups. Among CO's the alternation phenomenon is a consequence of the backbone structure: the electrostatically unfavorable, alternately axially antiparallel orientation of the groups. The dipoles of the neighboring carbonyls are oriented in opposing directions; their net dipole-dipole interaction energy is repulsive. To minimize repulsion (and increase overall channel stability) a large induced dipole moment in one group promotes a lower polarization of its neighbor. When the channel mouth is ion-free, electrostatic interaction between exo-carbonyls and nearby water molecules is attractive; that between the endo-carbonyls and water is repulsive. The average difference is $\approx$3 kJ mol^{-1} (1.2 k_BT) per group. In the helix interior, the aqueous electrostatic environment is fundamentally axially symmetric; dipole moment alternation leads to no reduction of energy.

For the NH's, the dipole moment pattern is a secondary consequence of the coordination of water by the exo-carbonyls. The hydrogen of the exo-NH is close to a water hydrogen, an energetically unfavorable arrangement. The dipolar interaction between that water molecule and NH is net repulsive, encouraging reduced polarization. The energetics of water-NH interaction complement the water-CO case. For an ion-free channel mouth, all exo-NH's are destabilized electrostatically and all endo-NH's are stabilized. The difference is much smaller, averaging only $\approx$0.5 kJ mol^{-1} (0.2 k_BT) per group.

Water dipoles

Incorporating polarizability has a marked effect on water's properties. Our results (Table 4) show that $\langle\mu\rangle$ for water molecules in an ion free channel is notably smaller than in bulk water. Even with Cs^+ in the channel the $\langle\mu\rangle$ for waters which do *not* neighbor the ion differ little from the value of an ion-free channel. The reduced dipole moments correlate qualitatively with the apparent lowered density of water in the channel environment. In bulk water, the volume per molecule is $\approx$30 Å^3. The interior of the channel is ~25 Å long and (depending upon how one measures) 2.1–2.4 Å in radius, a total volume of 350–450 Å^3; with an occupancy of only 7–9 single file waters, the density is from 50 to 70% of that in bulk. There is less water-water interaction and consequently, reduced water-water polarization (and a lower $\langle\mu\rangle$) in the channel is not unreasonable. Additionally, the peptide helix, unlike the molecules in bulk water, cannot reorganize as efficiently about the incorporated water molecules; the result would be reduced polarization. The effect would be reduced, but not eliminated, if alternating CO oxygens, as suggested by Chiu et al. (1989), exhibit more axial tilt than that indicated in Table 5, thus narrowing the channel.[10]

As already mentioned, the channel protein has greater charge separation than built into this model which could significantly lower the cation's free energy in the channel. Greater charge separation would also affect the water molecules in the channel. How this might influence $\langle\mu\rangle$ is unclear. However, it is known that changing the environment's capacity to induce polarization has a much greater influence on ions than on dipoles (Vayl and Jordan, 1987).

[10]It should be noted that a 2.1 Å radius (the lower bound used) already presumes substantial tilting.

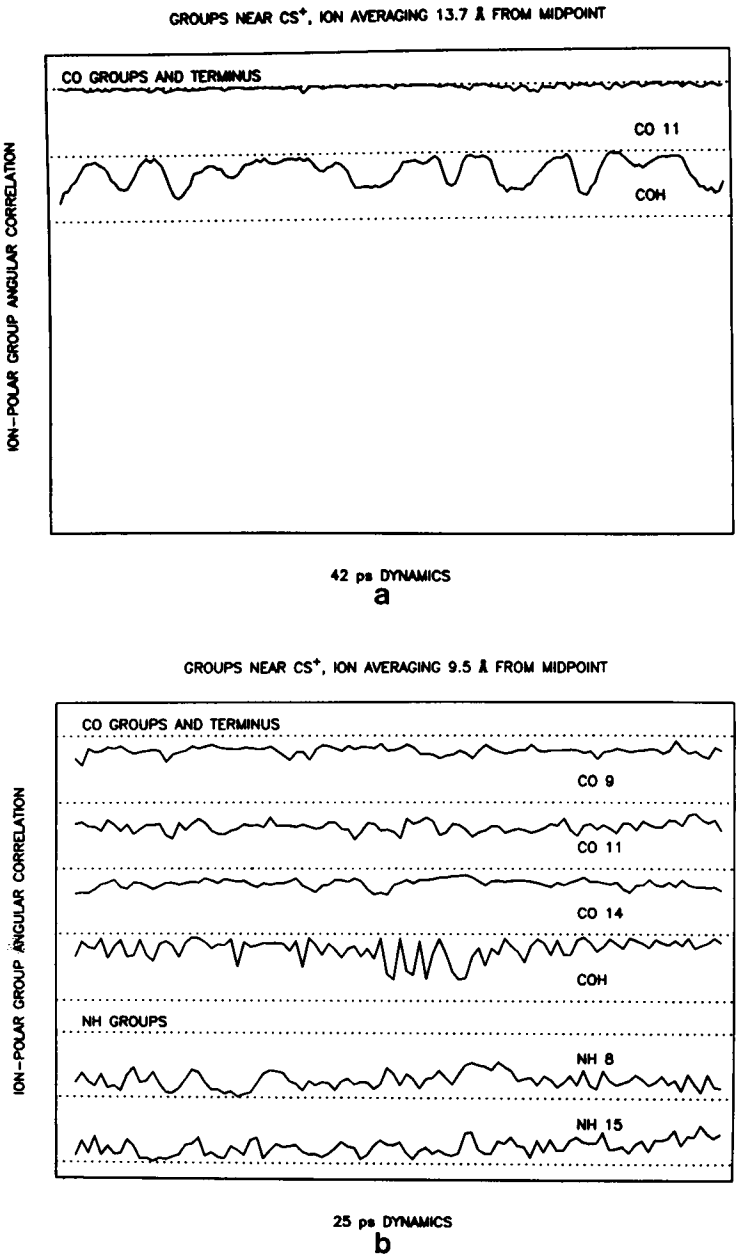

FIGURE 7 Dynamics of ion-dipole orientational correlation between an ion and its nearest neighbor polar groups at 300 K for the same regions described in Figs. 1 and 4: (*a*) Cs^+ near 13.7 Å; (*b*) Cs^+ near 9.5 Å; (*c*) Cs^+ near 0.5 Å; (*d*) Cl^- near 12.5 Å. The dotted lines indicate the values for which $\boldsymbol{n} \cdot \boldsymbol{u}_{i\to g} = \pm 1$ (see text); when $\boldsymbol{n} \cdot \boldsymbol{u}_{i\to g} = -1$ cation-carbonyl or anion-NH alignment is perfect.

Thus the effect on water dipoles is likely to be small; a more complete model should still exhibit lowered water dipole moments in the channel.

Single filing and pore occupancy

As shown in Figs. 2 and 3, water motion is highly correlated, a feature of all previous studies (Mackay et al., 1984; Skerra and Brickmann, 1987*a*, *b*; Chiu et al., 1989). If the single file region is defined by water molecules not in direct contact with any bulk water, it is seven molecules long. The water molecules in the mouths are in contact with bulk water. If they cannot exchange because they are constrained to the neighborhood of the channel axis by strong solvation interaction with the exo-carbonyls, the number in the single file is nine. Both

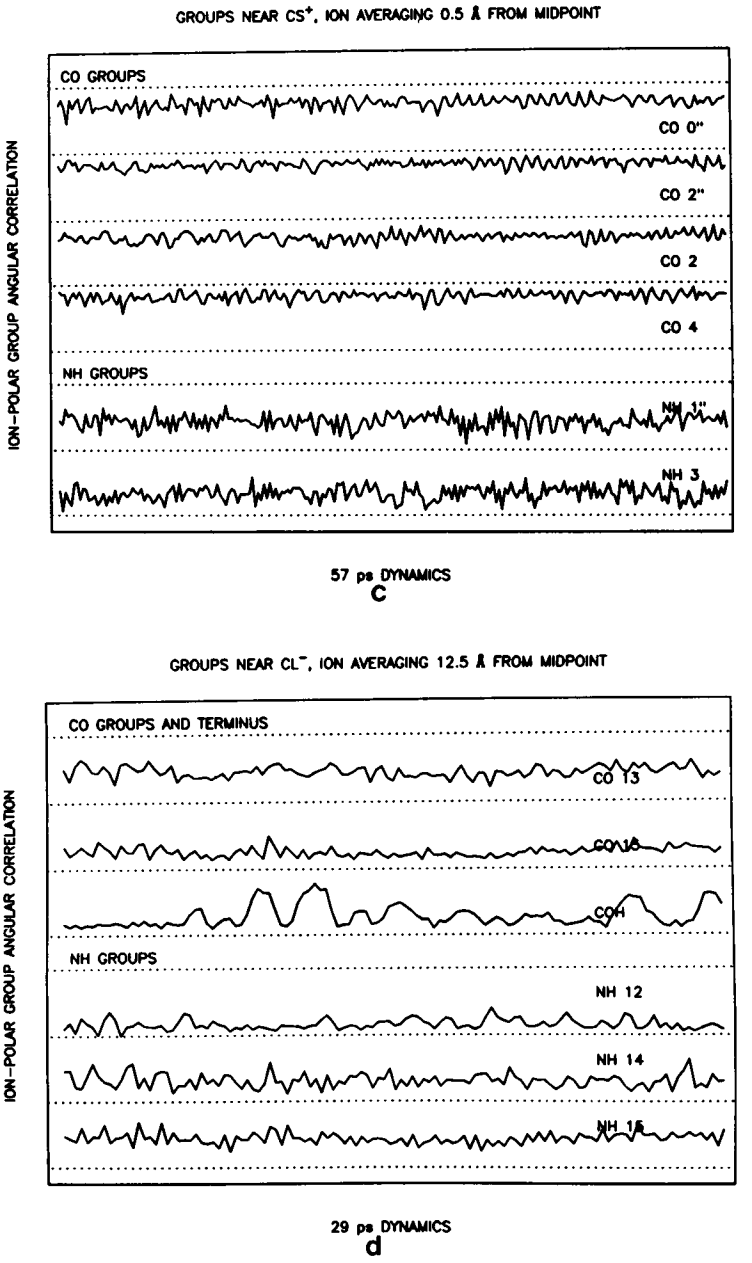

FIGURE 7 (continued)

classifications are consistent with the low salt concentration streaming potential estimates of 7-9 (Rosenberg and Finkelstein, 1978; Levitt, 1984). Depending upon which definition is used, this region extends either $\approx \pm 10$ or ± 12 Å to either side of the dimer junction. However, the single file, functionally, is those water molecules that translocate in conjunction with an ion during the permeation process, a period typically $\approx$10–100 ns (Andersen and Procopio, 1980). Thus, short time dynamics (<50 ps) on an ion-free channel is 1,000 times too short to definitively establish whether the water molecules in the channel mouth are also part of the single file.

With either Cs^+ or Cl^- in the permeation pathway, one water of the single file has been replaced; for dynamical runs varying from 25 to 60 ps, the total number of correlated waters is either eight or nine. However, two may be in direct contact with bulk water. During the translocation process contact with the bulk is occasionally

broken in one of the mouths and correlation of the extra water no longer persists. With Cs^+ as the permeant ion, in every window studied, the minimum number of correlated water molecules is seven, indicating that the single file comprises seven waters, an estimate consistent with previous theoretical and experimental results for larger cations (Skerra and Brickmann, 1987*a*; Levitt, 1984).

The length of the single file is determined in a way that differs sharply from that used by Skerra and Brickmann (1987*a*). They model gramicidin as a 22.9 Å segment of an infinite periodic helix of pitch 4.58 Å with 6 carbonyl units per turn and study water pair correlations as water molecules are added to the repeating unit (the unit contains a single ion). Their analysis shows an abrupt change in correlation function when water occupancy exceeds a critical value. This value is identified with the channel's single file capacity; with smaller ions, Li^+ or Na^+ as permeants, the water occupancy is 8 whereas for the larger ion, K^+, it is 7. The estimate of 7 given here is not strictly comparable as the ion, Cs^+, is somewhat larger. The models differ; here each ionic location is unique and the channel more closely resembles gramicidin. Single file structure varies as the ion translocates through the channel; in many configurations both mouth water molecules are part of the single file. However, regardless of ion location, the *minimum* number of correlated waters is seven.

Water-water and ion-water orientational correlations

Unlike previous studies (Mackay et al., 1984; Chiu et al., 1989), there are no persistent orientational correlations propagating the length of the channel. In the absence of ions water-water angular correlation at each channel terminus is controlled by the carbonyl groups at the mouth of the channel. With ions present, they naturally exert control. Structure propagates about two molecules from the ion or from a mouth, not to the channel's other side. Correlation appears to extend no further. With Cs^+ at the channel center, the picture is dramatically different. The channel mouth and the ion act in concert and dipolar preferences propagate in both directions. However, the pattern is still consistent with the idea that water mediated dipolar correlation extends for two waters only.

Why these predictions differ from those of previous dynamical studies (Mackey et al., 1984; Chiu et al., 1989) is unclear. There are a number of possibilities. None of the simulations is of truly long duration; thus all three studies may sample sharply different regions of the phase space of water configurations. More likely the divergent results are model based. The earlier force fields are quite similar to each other but not to ours. Neither includes the influence of polarizability; in particular, all water molecules are electrically identical, regardless of local environment. However, they use atom based force fields with charge separation, a feature not incorporated here.

The differences are compatible with our finding that polarizable channel waters have smaller dipole moments than water molecules in bulk. Both water-water and water-carbonyl electrostatic attractions are weaker than the corresponding quantities would be for "bulk-like" water molecules. The polarizable water molecules with their relatively small dipole moments are less likely to be orientationally ordered by their immediate surroundings than molecules with "bulk-like" properties; the consequence is limited persistence of dynamical angular correlations. In contrast, in the previous studies the intrinsic electrical properties of the water molecules are not influenced by the local environment; the channel waters have relatively high dipole moments and would exhibit too much orientational ordering.

However, the differences are equally compatible with the possibility that greater charge separation would promote stronger water-carbonyl interaction. Taking this viewpoint, the forces which promote local orientational stabilization may be significantly underestimated. Consequently, dynamical angular correlation could be notably more persistent.

Experiment provides an uncertain guide to discriminating between these possibilities. Correlated water mobility in the gramicidin channel is substantially less than in bulk, possibly by an order of magnitude (Dani and Levitt, 1981); however, individual waters diffuse as easily as in bulk. This is indicative of coupled motion, but not necessarily of persistent orientational correlation the length of the channel (with strong water-carbonyl interaction throughout). Whereas our calculations suggest that orientational correlations within the channel are not of long duration, those at the mouth are. Reduced water mobility may be a consequence of strong water-carbonyl interaction at the channel mouths even though the corresponding interactions within the channel may be relatively weak. The reduced mobility could also reflect steric limitations on water flow through the channel. The high degree of localization of water molecules observed in Fig. 2 and by previous studies (Mackay et al., 1984; Chiu et al., 1989) is certainly consistent with this interpretation. Molecular mechanics studies of two and four water molecules in the channel also suggest the existence of preferred sites for water binding (Sung and Jordan, 1987).

Ion-helix correlation

In an ion-free helix (Fig. 6 *a*) there is a general pattern of alternation of the angular deflections of the CO groups reflecting the fact, predicted by Urry (1971) and observed

by Mackay et al. (1984), that inward deflection of one CO creates a structural perturbation promoting outward deflection of its neighboring CO's. However, the alternation is gradual and the mean deflections are small (Table 5). These results contrast sharply with those presented by Chiu et al. (1989) where neighboring NH groups exhibit a distinct pattern of alternation and the carbonyl groups systematically tilt toward the channel axis. These differences are almost certainly model based and may reflect the influence of the group localization term in the potential function.

With Cs^+ present the deflection pattern is much perturbed. The *differential* deflection of the CO groups (the difference between a CO group's mean angular deflection in an occupied channel and the corresponding quantity in an ion-free channel) is large in the vicinity of the ion (Figs. 6, *b* and *c*). In magnitude, the maximum difference is somewhat less than that found by Mackay et al. (1984), but in contrast to that work, there is only slight additional alternation.

The orientational correlation between the ion and its nearest neighbor polar groups illustrated in Fig. 7 exhibits some important features. CO-Cs^+ alignment is notably stronger than CO-Cl^- alignment; orientational ordering with NH is less pronounced, reflecting reduced polarity. There is little direct interaction with COH of the ethanolamine residue, indicated by sporadic misalignments. In the channel mouth Cs^+ is nearly perfectly aligned with CO #11. In the interior, the helix cannot deform sufficiently to permit similar ideal alignment with two or more groups.

Ion coordination

An ion's solvation structure changes dramatically as it enters the channel. In the interior of the single file it binds, on average, ≈3 cabonyl groups in each region as it shuttles among ligands. Table 6 indicates this by distinguishing between those CO's for which the Cs^+-oxygen distance averages ≤3.3 Å and those with which it is more weakly associated (separations >3.3 and ≤4.0 Å); this is a slightly different description of ion-oxygen interaction than the coordination condition. Near the dimer junction the ion is tightly bound to four carbonyls simultaneously; this may account for increasing stability in this region, a property of many calculated PMF's (Mackay, D. H. J., P. M. Edelstein, and K. R. Wilson, unpublished results; Jordan, 1988; Åqvist and Warshel, 1989). In all other regions of the model channel the helix is not flexible enough to permit close and persistent association with more than two CO's even though in each configuration the ion is liganded by at least four carbonyls. Just inside the entrance barrier, near 9.5 Å, Cs^+ binds strongly to CO's 9 and 14 and interacts more weakly with CO's 11 and 12 and with the ethanolamine COH. Similar behavior is found throughout the channel. All local solvation structures are the same as those noted in our energy minimization studies (Lee and Jordan, 1984; Sung and Jordan, 1987) or by others (Åqvist and Warshel, 1989). Preliminary studies indicate that they do not change if the group localization constraint is released; however, in that case, more CO's are strongly bound and fewer are weakly associated.

As Cs^+ enters the channel, it remains close to the ethanolamine COH, even though, due to competitive interaction with water, orientational correlation (as noted in Fig. 7) may be far from optimal. Apparently the tail's unusual flexibility permits the ion to remain hexacoordinate until it is unambiguously in the interior single file. Of possibly greater interest is the association of Cs^+ with CO-11, which extends over 5 Å, a correlation distance greater than that of any other carbonyl. Not only is interaction with this carbonyl predominant when the ion is at the binding site, which we locate near 13.5 Å; it persists as the ion enters the channel. This is consistent with the unusually large chemical shift observed at that carbonyl in ^{13}C NMR studies (Urry et al., 1982*a*). Surprisingly, as is clear from Table 6, when the ion is in the vicinity of the binding site it *never* associates strongly with CO-15 but does interact effectively with CO-13 and the ethanolamine COH; the association with the tail localizes the ion in a way that it can bind to CO-13 but not to CO-15. Interaction with CO-9 does not become important until the ion has nearly surmounted the entrance barrier; it is therefore energetically improbable. Thus we expect weak chemical shifts at CO's 9 and 15 and large ones at CO's 11 and 13, consistent with the NMR data.

The model potential, with a group localization term that constrains helix deformation, reduces group mobility. This limits the helix's coordinating ability and the coordination number estimates may be a bit low. Releasing the constraint permits somewhat closer ion-CO association. However, the general coordination trends during translocates are potential independent. Preliminary calculations indicate that increased backbone flexibility has its greatest effect if Cs^+ is near the dimer junction. In the middle of the channel Cs^+ may well coordinate more than six ligands (including water); however, throughout most of the interior single file the ion is only pentacoordinate.

SUMMARY

Ionic interaction with a gramicidin-like channel (the polyglycine analogue) based upon interaction between polarizable, multipolar groups has been analyzed. The model suggests that the vicinity of the dimer junction and of the ethanolamine tail are regions of unusual flexibility.

Cation coordination changes dramatically as the ion translocates through the channel. In the mouth Cs^+ is hexacoordinate and binds at a weakly articulated site. It is solvated by five water molecules and interacts strongly with and is ideally aligned by the CO-11 group. As Cs^+ enters the interior single file of the channel its coordination number decreases from six to five. However, at the channel midpoint, because of flexibility at the dimer junction, the ion again becomes essentially hexacoordinate. In the vicinity of the binding site, in addition to its strong coupling with the CO-11, the ion interacts with CO-13 and the ethanolamine COH, but not with CO-15, consistent with the ^{13}C-NMR data (Urry et al., 1982*a*).

Water in the channel interior is strikingly different from bulk water; it has a much lower mean dipole moment. This correlates with the observation (which contrasts with that of previous studies (Mackay et al., 1984; Chiu et al., 1989) that water-water angular correlations do not persist within the channel, a result independent of ion occupancy or ionic polarity. There appear to be seven single file water molecules associated with Cs^+ permeation, consistent with experiment (Levitt, 1984) and previous theory (Skerra and Brickmann, 1987*a*); one of these is always in contact with bulk water. In many configurations there is an eighth water in the single file, associated with the bulk water at the other mouth of the channel.

At the channel mouth, there is a pattern of dipole moment alternation among the polar groups. Due to differential interaction with water, exo-carbonyls have unusually large dipole moments while those of the endo-carbonyls are low.

The computed potential of mean force, while qualitatively reasonable, exhibits far too high energy barriers with respect to bulk water and only a weakly articulated binding site. Correction for membrane polarization reduces, but does not eliminate, the problems. The general structure of the PMF is consistent with that found by most others, a well-defined entrance barrier followed by a minimum, an interior maximum near 6–7 Å from the channel midpoint and a minimum near the channel center.

I wish to thank E. Jakobsson, S. Subramanian, and S.-S. Sung for their suggestions during the preliminary stages of this study. I especially appreciate both D. Busath's critique of the preliminary manuscript and the thoughtful suggestions of the referees.

This work has been supported by grant GM-28643 from the National Institutes of Health (NIH), by instrument grants from both the NIH and the National Science Foundation (NSF) and by an allocation of time by the Pittsburgh Supercomputer Center. It was begun during a sabbatical leave at the University of Houston and partially supported, at that time, by grants to Prof. J. A. McCammon from the NIH, the NSF, and the Robert A. Welch Foundation.

Received for publication 20 November 1989 and in final form 4 June 1990.

REFERENCES

Andersen, O. S. 1984. Gramicidin channels. *Annu. Rev. Physiol.* 46:531–548.

Andersen, O. S., and J. Procopio. 1980. Ion movement through gramicidin channels. *Acta Physiol. Scand. Suppl.* 481:27–35.

Andersen, O. S., J. T. Durkin, and R. E. Koeppe II. 1988. Do amino acid substitutions alter the structure of gramicidin channels? Chemistry at the single molecule level. *In* Transport through Membranes: Carriers, Channels, and Pumps. A. Pullman, B. Pullman, and J. Jortner, editors. Kluwer Academic Publishers, Dordrecht, Netherlands. 115–132.

Andersen, O. S., L. L. Providence, and R. E. Koeppe II. 1990. Gramicidin channels are right-handed β-helical dimers. *Biophys. J.* 57:100*a*. (Abstr.)

Åqvist, J., and A. Warshel. 1989. Energetics of ion permeation through gramicidin channels. Solvation of Na^+ by gramicidin A. *Biophys. J.* 56:171–182.

Arseniev, A. S., I. L. Barsukov, V. F. Bystrov, A. L. Lomize, and Yu. A. Ovchinnikov. 1985. ^{1}H-NMR study of gramicidin A transmembrane ion channel. Head-to-head, right-handed, single-stranded helices. *FEBS (Fed. Eur. Biochem. Soc.) Lett.* 186:168–174.

Bamberg, E., and P. Läuger. 1974. Temperature dependent properties of gramicidin A channels. *Biochim. Biophys. Acta.* 552:369–378.

Bamberg, E., K. Noda, E. Gross, and P. Läuger. 1976. Single channel parameters of gramicidin A, B and C. *Biochim. Biophys. Acta.* 418:223–228.

Barnes, P., J. L. Finney, J. D. Nicholas, and J. E. Quinn. 1979. Cooperative effects in simulated water. *Nature (Lond.).* 282:459–464.

Barrett-Russell, E. W., L. B. Weiss, F. I. Navetta, R. E. Koeppe II, and O. S. Andersen. 1986. Single-channel studies on linear gramicidins with altered amino acid sequences. Effects of altering the polarity of the side chain at position 1 in gramicidin A. *Biophys. J.* 49:673–686.

Berendsen, H. J. C., J. P. M. Postma, W. F. van Gunsteren, A. DiNola, and J. R. Haak. 1985. Molecular dynamics with coupling to an external bath. *J. Chem. Phys.* 81:3684–3690.

Brooks, B. R., R. E. Bruccoleri, B. D. Olafson, D. J. States, S. Swaminathan, and M. Karplus. 1983. CHARMM: A program for macromolecular energy, minimization, and dynamics calculations. *J. Comp. Chem.*, 4:187–217.

Chiu, S. W., and E. Jakobsson. 1989. Stochastic theory of singly occupied ion channels. II. Effects of access resistance and potential gradients extending into the bath. *Biophys. J.* 55:147–157.

Chui, S. W., S. Subramanian, E. Jakobsson, and J. A. McCammon. 1989. Water and polypeptide conformations in the gramicidin channel. A molecular dynamics study. *Biophys. J.* 56:253–261.

Cornell, B. A., and F. Separovic. 1989. Conformation and order of gramicidin A in phospholipid dispersions. *Biophys. J.* 55:504*a* (Abstr.).

Cornell, B. A., F. Separovic, A. J. Baldassi, and R. Smith. 1988. Conformation and orientation of gramicidin A in oriented phospholipid bilayers measured by solid state carbon-13 NMR. *Biophys. J.* 53:67–76.

Dani, J. A., and D. G. Levitt. 1981. Water transport and ion-water interaction in the gramicidin channel. *Biophys. J.* 35:501–508.

DeGrado, W. F., Z. R. Wasserman, and J. D. Lear. 1989. Protein design, a minimalist approach. *Science (Wash. DC).* 243:622–628.

Durkin, J. T., O. S. Andersen, E. R. Blout, F. Heitz, R. E. Koeppe, II, and Y. Trudelle. 1986. Structural information from functional measurements. Single-channel studies of gramicidin analogues. *Biophys. J.* 49:118–121.

Durkin, J. T., O. S. Andersen, F. Heitz, Y. Trudelle, and R. E. Koeppe II. 1987. Linear gramicidins can form channels that do not have the $\beta^{6.3}$ structure. *Biophys. J.* 51:451*a* (Abstr.)

Eisenman, G., and J. P. Sandblom. 1983. Energy barriers in ionic channels: data for gramicidin A interpreted using a single-file (3B4S″) model having 3 barriers separating 4 sites. *In* Physical Chemistry of Transmembrane Ion Motions. G. Spach, editor. Elsevier North-Holland, Amsterdam. 329–347.

Etchebest, C., and A. Pullman. 1984. The gramicidin A channel. Role of the ethanolamine end chain on the energy profiles for single occupancy by Na^+. *FEBS (Fed. Eur. Biochem. Soc.) Lett.* 170:191–195.

Etchebest, C., and A. Pullman. 1986. The gramicidin A channel. The energy profile calculated for Na^+ in the presence of water with inclusion of the flexibility of the ethanolamine tail. *FEBS (Fed. Eur. Biochem. Soc.) Lett.* 204:261–265.

Etchebest, C., and A. Pullman. 1988. The gramicidin A channel: left versus right handed helix. *In* Transport through Membranes: Carriers, Channels and Pumps. A. Pullman, B. Pullman, and J. Jortner, editors. Kluwer Academic Publishers, Dordrecht, Netherlands. 167–185.

Etchebest, C., S. Ranganathan, and A. Pullman. 1984. The gramicidin A channel: comparison of the energy profiles of Na^+, K^+, and Cs^+. Influence of the flexibility of the ethanolamine end chain on the profiles. *FEBS (Fed. Eur. Biochem. Soc.) Lett.* 173:301–306.

Evans, D. J., and S. Murad. 1977. Singularity free algorithm for molecular dynamics simulation of rigid polyatomics. *Mol. Physiol.* 34:327–331.

Fischer, W., J. Brickmann, and P. Läuger. 1981. Molecular dynamics study of ion transport in transmembrane protein channels. *Biophys. Chem.* 13:105–116.

Fornili, S. L., D. P. Vercauteren, and E. Clementi. 1984. Water structure in the gramicidin A transmembrane channel. *Biochim. Biophys. Acta.* 771:151–164.

Gear, C. W. 1971. *Numerical Initial Value Problems in Ordinary Differential Equations.* Prentice Hall, Englewood Cliffs, NJ. 136–157.

Gowda, B. T., and S. W. Benson. 1982. Empirical potential parameters for alkali halide molecules and crystals, hydrogen halide molecules, alkali metal dimers and hydrogen and halogen molecules. *J. Phys. Chem.* 86:847–857.

Heitz, F., G. Spach, and Y. Trudelle. 1982. Single channels of 9, 11, 13, 15-destryptophyl-phenylanalyl-gramicidin A. *Biophys. J.* 40:87–89.

Heitz, F., C. Gavach, and Y. Trudelle. 1984. Single channels of various gramicidins. Voltage effects. *Biophys. J.* 45:97–99.

Hermans, J., H. J. C. Berendsen, W. F. van Gunsteren, and J. P. M. Postma. 1984. A consistent empirical potential for water-protein interactions. *J. Comp. Chem.* 23:1513–1518.

Hille, B. 1984. Ionic Channels of Excitable Membranes. Sinauer Associates, Inc., Sunderland, MA. 226–271.

Hladky, S. and D. A. Haydon. 1972. Ion transfer across lipid bilayer membranes in the presence of gramicidin A. Studies of the unit conductance channel. *Biochim. Biophys. Acta.* 274:294–312.

Hladky, S., and D. A. Haydon. 1973. Membrane conductance and surface potential. *Biochim. Biophys. Acta.* 318:464–468.

Jakobsson, E., and S. W. Chiu. 1987. Stochastic theory of ion movement in channels with single-ion occupancy. Application to sodium permeation of gramicidin channels. *Biophys. J.* 52:33–45.

Jonsson, B., O. Edholm, and O. Teleman. 1986. Molecular dynamics simulations of a sodium octanoate micelle in aqueous solution. *J. Chem. Phys.* 85:2259–2271.

Jordan, P. C. 1982. Electrostatic modeling of ion pores. Energy barriers and electric field profiles. *Biophys. J.* 39:157–164.

Jordan, P. C. 1983. Electrostatic modeling of ion pores. II. Effects attributable to the membrane dipole potential. *Biophys. J.* 41:189–195.

Jordan, P. C. 1984. The total electrostatic potential in a gramicidin channel. *J. Membr. Biol.* 78:91–102.

Jordan, P. C. 1987. Microscopic approaches to ion transport through transmembrane channels. The model system gramicidin. *J. Phys. Chem.* 91:6582–6591.

Jordan, P. C. 1988. A molecular dynamics study of cesium ion motion in a gramicidin-like channel. Structural and energetic implications. *In* Transport through Membranes: Carriers, Channels and Pumps. A. Pullman, B. Pullman, and J. Jortner, editors. Kluwer Academic Publishers, Dordrecht, Netherlands. 237–251.

Kim, K. S., and E. Clementi. 1985. Energetics and hydration structures of a solvated gramicidin A transmembrane channel for K^+ and Na^+ cations. *J. Am. Chem. Soc.* 107:5504–5513.

Kim, K. S., D. P. Vercauteren, M. Welti, S. Chin, and E. Clementi. 1985. Interaction of K^+ ion with solvated gramicidin A transmembrane channel. *Biophys. J.* 47:327–335.

Koeppe, R. E. II, and M. Kimura. 1984. Computer building of β-helical polypeptide models. *Biopolymers.* 23:23–38.

Koeppe, R. E. II, O. S. Andersen, and A. K. Maddock. 1988. How do amino acid substitutions alter the function of gramicidin A channels? *In* Transport through Membranes: Carriers, Channels and Pumps. A. Pullman, B. Pullman, and J. Jortner, editors. Kluwer Academic Publishers, Dordrecht, Netherlands. 133–145.

Kong, C. L. 1973. Combining rules for intermolecular potential parameters. II. Rules for the Lennard-Jones (12,6) potential and Morse potential. *J. Chem. Phys.* 59:2464–2467.

Koyama, Y., and T. Shimanouchi. 1974. An experimental study of the internal rotation potentials about the N-C and C-C′ axes of the peptide backbone. *In* Peptides, Polypeptides and Proteins. F. R. Blout, F. A. Bovey, M. Goodman, and N. Lotan, editors. John Wiley and Sons, Inc., New York. 396–418.

Landau, L. D., and E. M. Lifschitz. 1960. Electrodynamics of Continuous Media. Pergamon Press, Oxford. 253–256.

Lee, C. Y., J. A. McCammon, and P. J. Rossky. 1984. The structure of liquid water at an extended hydrophobic surface. *J. Chem. Phys.* 80:4448–4455.

Lee, W. K., and P. C. Jordan. 1984. Molecular dynamics simulation of cation motion in water-filled gramicidinlike pores. *Biophys. J.* 46:805–819.

Levitt, D. G. 1984. Kinetics of movement in narrow channels. *In* Ion Channels: Molecular and Physiological Aspects. W. D. Stein, editor. Academic Press, New York. 181–197.

Lin, S., and P. C. Jordan. 1988. Structures and energetics of monovalent ion-water microclusters. II. Thermal Phenomena. *J. Chem. Phys.* 89:7492–7501.

Lybrand, T. P., J. A. McCammon, and G. Wipff. 1986. Theoretical calculations of relative binding affinity in host-guest systems. *Proc. Natl. Acad. Sci. USA.* 83:833–835.

Mackay, D. H. J., P. H. Berens, K. R. Wilson, and A. T. Hagler. 1984. Structure and dynamics of ion transport through gramicidin-A. *Biophys. J.* 46:229–248.

Mazet, J. L., O. S. Andersen, and R. E. Koeppe, II. 1984. Single-channel studies on linear gramicidins with altered amino acid sequences. A comparison of phenylalanine, tryptophane and tyrosine substitutions at positions 1 and 11. *Biophys. J.* 45:263–276.

McCammon, J. A., P. G. Wolnyes, and M. Karplus. 1979. Picosecond dynamics of tyrosine side chains in proteins. *Biochemistry.* 18:927–942.

McQuarrie, D. A. 1976. Statistical Mechanics. Harper and Row, New York. 116.

Neumann, D. and J. W. Moskowitz. 1968. One-electron properties of near-Hartree-Fock wave functions. I. Water. *J. Chem. Phys.* 49:2056–2070.

Nicholson, L. K., and T. A. Cross. 1989. Gramicidin cation channel: an experimental determination of the right-handed helix sense and verification of β-type hydrogen bonding. *Biochemistry.* 28:9379–9385.

Noda, M., H. Takahashi, T. Tanabe, M. Toyosato, S. Kikyotani, Y. Furutani, T. Hirose, H. Takashima, S. Inayama, T. Miyata, and S. Numa. 1983. Structural homology of *Torpedo californica* acetylcholine receptor subunits. *Nature (Lond.).* 302:528–532.

Noda, M., S. Shimizu, T. Tanabe, T. Takai, T. Kayano, T. Ikeda, H. Takahashi, H. Nakayama, Y. Kanaoka, N. Minamino, K. Kangawa, H. Matsuo, M. A. Raftery, T. Hirose, S. Inayama, H. Hayashida, T. Miyata, and S. Numa. 1984. Primary structure of *Electrophorus electricus* sodium channel deduced from cDNA sequence. *Nature (Lond.).* 312:121–127.

Oiki, S., W. Danho, V. Madison, and M. Montal. 1988. M2 δ, a candidate for the structure lining the ionic channel of the nicotinic cholinergic receptor. *Proc. Natl. Acad. Sci. U.S.A.* 85:8703–8707.

Paltauf, F., H. Hauser, and M. C. Phillips. 1971. Monolayer characteristics of some 1,2-diacyl, 1-alkyl-2-acyl and 1,2-dialkyl phospholipids at the air-water interface. *Biochim. Biophys. Acta.* 249:539–547.

Pangali, C. S., M. Rao, and B. J. Berne. 1979. A Monte Carlo simulation of the hydrophobic interaction. *J. Chem. Phys.* 71:2975–2981.

Pethig, R. 1979. Dielectric and Electronic Properties of Biological Materials. John Wiley and Sons, Inc., Chichester, England.

Pickar, A. D., and R. Benz. 1978. Transport of oppositely charged lipophilic probe ions in lipid bilayer membranes having various structures. *J. Membr. Biol.* 44:353–376.

Polymeropoulos, E. E., and J. Brickmann. 1985. Molecular dynamics of ion transport through transmembrane model channels. *Ann. Rev. Biophys. Biophys. Chem.* 14:315–330.

Pullman, A. 1987. Energy profiles in the gramicidin channel. *Quart. Rev. Biophys.* 20:173–200.

Pullman, A., and C. Etchebest. 1983. The gramicidin A channel: the energy profile for single and double occupancy in a head-to-head $\beta_3^6, {}^3_3$ helical dimer backbone. *FEBS (Fed. Eur. Biochem. Soc.) Lett.* 163:199–202.

Rosenberg, P. A., and A. Finkelstein. 1978. Interaction of ions and water in gramicidin A channels. Streaming potentials across lipid bilayer membranes. *Biophys. J.* 27:455–460.

Shepard, A. C., Y. Beers, G. P. Klein, and L. S. Rothman. 1973. Dipole moment of water from Stark measurements of H_2O, HDO, and D_2O. *J. Chem. Phys.* 59:2254–2259.

Skerra, A., and J. Brickmann. 1987*a*. Structure and dynamics of one-dimensional solutions in biological transmembrane channels. *Biophys. J.* 51:969–976.

Skerra, A., and J. Brickmann. 1987*b*. Simulation of voltage-driven hydrated cation transport through narrow transmembrane channels. *Biophys. J.* 51:977–983.

Stühmer, W., F. Conti, H. Suzuki, X. Wang, M. Noda, N. Yahagi, H. Kubo, and S. Numa. 1989. Structural parts involved in activation and inactivation of the sodium channel. *Nature (Lond.).* 339:597–603.

Sung, S. S., and P. C. Jordan. 1986. Structures and energetics of monovalent ion-water microclusters. *J. Chem. Phys.* 85:4045–4051.

Sung, S. S., and P. C. Jordan. 1987. Why is gramicidin valence selective? A theoretical study. *Biophys. J.* 51:661–672.

Urban, B. W., S. B. Hladky, and D. A. Haydon. 1980. Ion movements in gramicidin pores. An example of single-file transport. *Biochim. Biophys. Acta.* 602:331–354.

Urry, D. W. 1971. The gramicidin A transmembrane channel. A proposed ($\pi_{L,D}$) helix. *Proc. Natl. Acad. Sci. U.S.A.* 68:672–676.

Urry, D. W., C. M. Venkatachalam, A. Spisni, P. Läuger, and Md.A. Khaled. 1980. Rate theory calculation of gramicidin single-channel currents using NMR-derived rate constants. *Proc. Natl. Acad. Sci. U.S.A.* 77:2028–2032.

Urry, D. W., K. U. Prasad, and T. L. Trapane. 1982*a*. Location of monovalent cation binding sites in the gramicidin channels. *Proc. Natl. Acad. Sci. U.S.A.* 79:390–394.

Urry, D. W., J. T. Walker, and T. L. Trapane, 1982*b*. Ion interactions in (1-^{13}C)D-val^8 and D-leu^{14} analogs of gramicidin A, the helix sense of the channel and location of ion binding sites. *J. Membr. Biol.* 69:225–231.

Urry, D. W., S. Alonso-Romanoski, C. M. Venkatachalam, T. L. Trapane, R. D. Harris, and K. U. Prasad. 1984. Shortened analog of the gramicidin A channel argues for the doubly occupied channel as the dominant conducting state. *Biochim. Biophys. Acta.* 775:115–119.

van Gunsteren, W. F., and M. Karplus. 1982. Effects of constraints on the dynamics of macromolecules. *Macromol.* 15:1528–1544.

Vayl, I. S., and P. C. Jordan. 1987. Electrostatic modeling of ion pores. Multipolar sources. *Biophys. Chem.* 27:7–13.

Wallace, B. A. 1986. The structure of gramicidin A. *Biophys. J.* 49:295–306.

Wallace, B. A., and K. Ravikumar. 1988. The gramicidin pore: crystal structure of a cesium complex. *Science (Wash. DC).* 241:182–187.

Warshel, A., and S. T. Russell. 1984. Calculations of electrostatic interactions in biological systems and in solutions. *Q. Rev. Biophys.* 17:283–422.

Weiner, S. J., P. A. Kollman, D. A. Case, U. C. Singh, C. Ghio, G. Alagona, S. Profeta, Jr., and P. Weiner. 1984. A new force field for molecular mechanical simulation of nucleic acids and proteins. *J. Am. Chem. Soc.* 106:756–784.